

Master's Programme in Advanced Energy Solutions

Verification and Validation of Passive Heat Removal Systems' Simulation Models

Topias Ali Zein

Master's Thesis
2021

The document can be stored and made available to the public on the open internet pages of Aalto University. All other rights are reserved.

Copyright ©2021 Topias Zein

Author Topias Ali Zein

Title of thesis

Verification and Validation of Passive Heat Removal Systems' Simulation Models

Programme ELEC26 - Advanced Energy Solutions

Major ELEC3048 - Sustainable Energy Systems and Markets

Thesis supervisor Prof. Ahti Salo

Thesis advisor(s) Calle Korhonen, M.Sc. (Tech.)

Collaborative partner Fennovoima Oy

Date 29.09.2021

Number of pages 88+10

Language EN

Abstract

Deterministic safety analyses are performed in the nuclear industry to ensure that the plant in question can withstand certain postulated events. To study how the plant is affected by such transients or accidents, analyses are made using specialised software. This computer simulation program, a model of the nuclear power plant is constructed to simulate the behaviour of the facility. The results of these analyses, however, depend on the accuracy of the model. As nuclear safety is the most important factor in the nuclear industry, it is essential to ensure that the model used for safety analyses is accurate and models the plant correctly. This is the process called verification and validation.

In this thesis, a verification and validation process is performed to two individual parts of the Hanhikivi-1 plant model, the passive heat removal systems of steam generator and of containment. These two were chosen because they are new safety systems unique to Generation III+ reactors and because commissioning test data is available for them from the Leningrad-II nuclear power plant. This real-world data allows to conduct a more reliable validation comparison.

The verification was done by studying the model and making preliminary calculations to test the functioning of the systems. As an outcome of this, model updates were made, and the heat convection correlation was changed to Churchill and Chu mixed free and forced convection. The validation study was made by comparing the results calculated in Apros with the results of the commissioning tests performed at Leningrad-II reference plant. The comparison showed that the results are analogous, and that the simulation model is accurate. It is suggested that further studies are performed with these systems as the data available was limited. Additionally, the rest of the model should be verified and validated if more data is made available from the reference plant.

Keywords verification, validation, passive heat removal system, Apros

Table of Contents

1	INTRODUCTION	11
2	VVER-1200 AND FH1	13
2.1	Hanhikivi-1 Nuclear Power Plant	13
2.2	Passive heat removal systems	15
2.2.1	Steam generator passive heat removal system (JNB)	16
2.2.2	Containment passive heat removal system (JMP)	19
3	APROS SIMULATION SOFTWARE	23
3.1	Neutronics	23
3.2	Thermal Hydraulics	25
3.2.1	Flow model 6	25
3.2.2	Convection heat transfer	27
3.3	Containment.....	30
4	HANHIKIVI-1 PLANT MODEL	32
4.1	Reactor	32
4.2	Primary side	32
4.3	Secondary side.....	34
4.4	Containment.....	35
4.5	Passive heat removal systems	36
4.5.1	Steam generator passive heat removal system	36
4.5.2	Containment passive heat removal system.....	40
5	VERIFICATION AND VALIDATION OF COMPUTER SIMULATION MODELS	43

5.1	Background	43
5.2	Definition.....	44
5.3	Processes	45
5.3.1	Conceptual model validation	46
5.3.2	Computerized model verification.....	47
5.3.3	Operational validation.....	48
6	RESEARCH METHODS.....	49
6.1	Verification methodology.....	49
6.2	Validation calculations.....	50
7	RESULTS.....	53
7.1	Steam generator passive heat removal system	53
7.1.1	Verification	53
7.1.2	Validation	58
7.2	Containment passive heat removal system	66
7.2.1	Verification	66
7.2.2	Validation	72
8	DISCUSSION.....	78
8.1	Steam generator passive heat removal system	78
8.2	Containment passive heat removal system	79
8.3	Limitations	80
8.4	Recommendations	81
8.5	Future work.....	82
9	CONCLUSIONS.....	83
	REFERENCES	85

Preface

This Master's Thesis was made at Fennovoima Oy in the Nuclear Safety department and I would like to thank the organisation for this opportunity.

Special thanks go to my supportive advisor, Calle Korhonen, and my colleagues Jukka Rintala and Janne Pitkänen for the help and guidance they provided throughout this project. Also, thanks to the rest of the Deterministic Safety Analysis unit and other colleagues from Fennovoima that aided me and shared their knowledge. From Aalto University's side, I would like to thank my supervisor Professor Ahti Salo for the invaluable advice and feedback he provided.

Finally, many thanks go to my girlfriend, family and friends for their encouragement and support.

Helsinki, September 29th, 2021

Topias Zein

SYMBOLS AND ABBREVIATIONS

Symbols

Latin

<i>A</i>	flow area	m ²
<i>B</i>	thermal expansion coefficient	-
<i>C</i>	concentration	ppm
<i>D</i>	neutron diffusion coefficients	cm
<i>d</i>	diameter	m
<i>F</i>	friction	N
<i>g</i>	gravitational acceleration	m/s ²
<i>h</i>	specific enthalpy	kJ/kg
<i>L</i>	length	m
<i>p</i>	pressure	Pa
<i>Q</i>	heat transfer rate	W
<i>S</i>	neutron emission rate	1/cm ³
<i>s</i>	sources of mass, momentum and energy	-
<i>T</i>	temperature	K
<i>t</i>	time	s
<i>u</i>	velocity of the fluid	m/s
<i>v</i>	neutron velocity	m/s
<i>w</i>	velocity of gas mixture in the node	m/s

Dimensionless quantities

<i>f</i>	Darcy friction factor
<i>Gr</i>	Grashof number
<i>Nu</i>	Nusselt number
<i>Pr</i>	Prandtl number
<i>Ra</i>	Rayleigh number
<i>Re</i>	Reynolds number

Greek

α	volume fraction	-
β	total fraction of delayed neutrons	pcm
Γ	mass transfer rate	kg/m ³ s
λ	decay constant	s
μ	dynamic viscosity	N s/m ²
ν	kinematic viscosity	m ² /s
ρ	density	kg/m ³
Σ	cross section	1/cm
ϕ	neutron flux	1/cm ² s

Subscripts

1	fast neutron
12	from fast to thermal neutron group
2	thermal neutron
∞	PHRS tank
B	bulk temperature
b1	absorption in fast neutron group
b2	absorption in thermal neutron group
f	fission
g	gas
i	phase i
i, k	between phases i and k
k	phase k
S	surface
w	wall
w, k	between wall and phase k
y	mass, momentum and energy

Operators

∇	divergence
$\frac{\delta}{\delta t}$	partial derivative with respect to variable t
Σ_j	sum over index j

Abbreviations

AOO	Anticipated Operational Occurrence
CPHRS	Containment Passive Heat Removal System
DBA/DBC	Design Basis Accident/Case
DEC	Design Extension Condition
FH1	Hanhikivi-1 Nuclear Power Plant
HE	Heat Exchanger
IAEA	International Atomic Energy Agency
LAES-II	Leningrad-II Nuclear Power Plant
LOCA	Loss-of-coolant accident
MSH	Main Steam Header
NPP	Nuclear Power Plant
PHRS	Passive Heat Removal System
PRISE	Primary-to-Secondary Leak
PSAR	Preliminary Safety Analysis Report
PWR	Pressurised Water Reactor
SA	Severe Accident
SG	Steam Generator
SG PHRS	Steam Generator Passive Heat Removal System
VVER	Water-Water Energetic Reactor
VTT	Technical Research Centre of Finland
V&V	Verification and Validation

1 INTRODUCTION

During all phases of a nuclear power plant's life, deterministic safety analyses are performed to study the possible transients and accidents that could occur at the plant and plan the safety systems to successfully handle these events. The events that are analysed are called Anticipated Operational Occurrences (AOO), Design Basis Accidents (DBA), Design Extension Conditions (DEC) and Severe Accidents (SA) on which the design of the plant and of the safety systems is built upon. If the plant is built to withstand all these postulated accidents, the risk of causing hazard to individuals and the environment is low.

To demonstrate that the facility is tolerant to certain identified accident scenarios, an accurate model of the plant is constructed. This model must precisely follow the functioning of the actual plant to ensure that the results of the analyses are correct and can be trusted upon. To make sure that the code used, and the model built are precise, a validation process must be conducted. Apros Nuclear as a code has been extensively verified and validated for various reactors, especially for VVER-440 by VTT and Fortum (Ylijoki et al., 2015).

The AES-2006 Hanhikivi-1 (FH1) Apros model has been in development since 2014. It has most of the plant modelled (Peltokorpi & Hongisto, 2020). The model includes a 1D and a 3D neutronics core model, primary circuit, secondary circuit, turbine, all important safety systems and safety automation and containment. Also, some main plant controllers are modelled. Regarding the passive heat removal systems (PHRS), the Steam Generator (SG) PHRS and the Containment PHRS are both modelled.

The FH1 model has been widely used for independent and own safety analyses by Fennovoima. Various comparative transients and accident scenarios

have been run with the model and compared with the plant Supplier's, RAOS Project Oy's (subsidiary of Rusatom Overseas, part of the Rosatom State Corporation Group) analyses. From the similarities of the analyses results, one can say that the model does indeed represent the plant accurately as long as the Supplier's model is precise. However, the model has not been formally verified and validated and as such, a verification and validation (V&V) is needed to be done.

The objective of this thesis is to perform a V&V for specific parts of the plant model. To limit the scope of this work appropriately, the Passive Heat Removal Systems of steam generators and of containment are studied. These were chosen because the PHRSs are a new type of safety system that has been implemented only in Gen III+ reactors (World Nuclear Association, 2020). Additionally, the Supplier has provided real-life data from SG and containment PHRS experiments and commissioning tests conducted at the LAES-II reference plant. With this data, the V&V process is simpler and more trustworthy as this data can be compared with Apros model data to find out the precision of the plant model.

The thesis consists of an introduction, background sections, a literature study, a research part, a results section and finally conclusions. In the introduction part, the background, the scope and the objectives of the thesis are presented. In the background sections, the type of power plant and its systems are described, and the code and model used are presented. Next, the different methods of V&V are outlined in the literature study. The research section includes the V&V methods chosen in this thesis in addition to the calculations performed to validate the model. In the results section the V&V is done using the methods presented in the previous chapter and finally the results and the V&V are summarised in the conclusions.

2 VVER-1200 AND FH1

VVER-1200 also known as AES-2006 is a Gen III+ pressurized water reactor designed in Russia by Rosatom, based on VVER technology. It is an evolution of the VVER-1000 with improved design in terms of efficiency, safety and lifetime (World Nuclear Association, 2021). Its specifications include a 54-month construction time, 60 years design lifetime, 90% capacity factor and 37% thermal efficiency as per Rosatom (2013). Moreover, there are two families of VVER-1200 designs: V-392M designed by Moscow Atomenergoproekt and V-491 by St Petersburg Atomenergoproekt. The most significant difference between these two designs are that the V-491 has a four times redundancy in most safety and control systems compared to the two times redundancy in the V-392M (State Atomic Energy Corporation ROSATOM, 2013). Both designs incorporate passive safety systems. Currently there are five operational VVER-1200 reactors, four in Russia and one in Belarus, and several in-construction around the world (World Nuclear Association, 2021).

2.1 Hanhikivi-1 nuclear power plant

The FH1 NPP that will be built on the Hanhikivi peninsula in Northern Ostrobothnia is a VVER-1200 V-522 which is the V-491 designed by St Petersburg Atomenergoproekt adapted to Finland (World Nuclear Association, 2020). It is a 1200 MWe, 3200 MWt 4-loop PWR with horizontal steam generators. The normal operating conditions of a VVER-1200 are coolant temperature of 298 °C at core inlet and 329 °C at core outlet and pressures of 16.2 MPa in the primary loop and 6.8 MPa in the main steam header (MSH) of the secondary side. The refuelling period is 12-18 months and the expected service life 60 years. (State Atomic Energy Corporation ROSATOM, 2013)

The reactor core of a VVER-1200 consists of 163 fuel assemblies in a hexagonal pattern and each fuel assembly has 252 fuel rods. The reactivity is

controlled using 121 control rods and using boron injected into the primary circuit. The fuel columns are 3.73 metres tall and have 13 spacer grids (including the anti-vibration one) distributed 34 centimetres apart. The weight of the uranium oxide fuel can be up to 534 kilograms and the enrichment up to 5 %. (State Atomic Energy Corporation ROSATOM, 2013)

As a Gen III+ reactor design, the VVER-1200 has all the conventional active safety systems and various passive ones. A simplified image of the main systems is in Figure 1. The figure is not drawn to scale, and the objects are not exactly at the correct locations when compared to the actual plant.

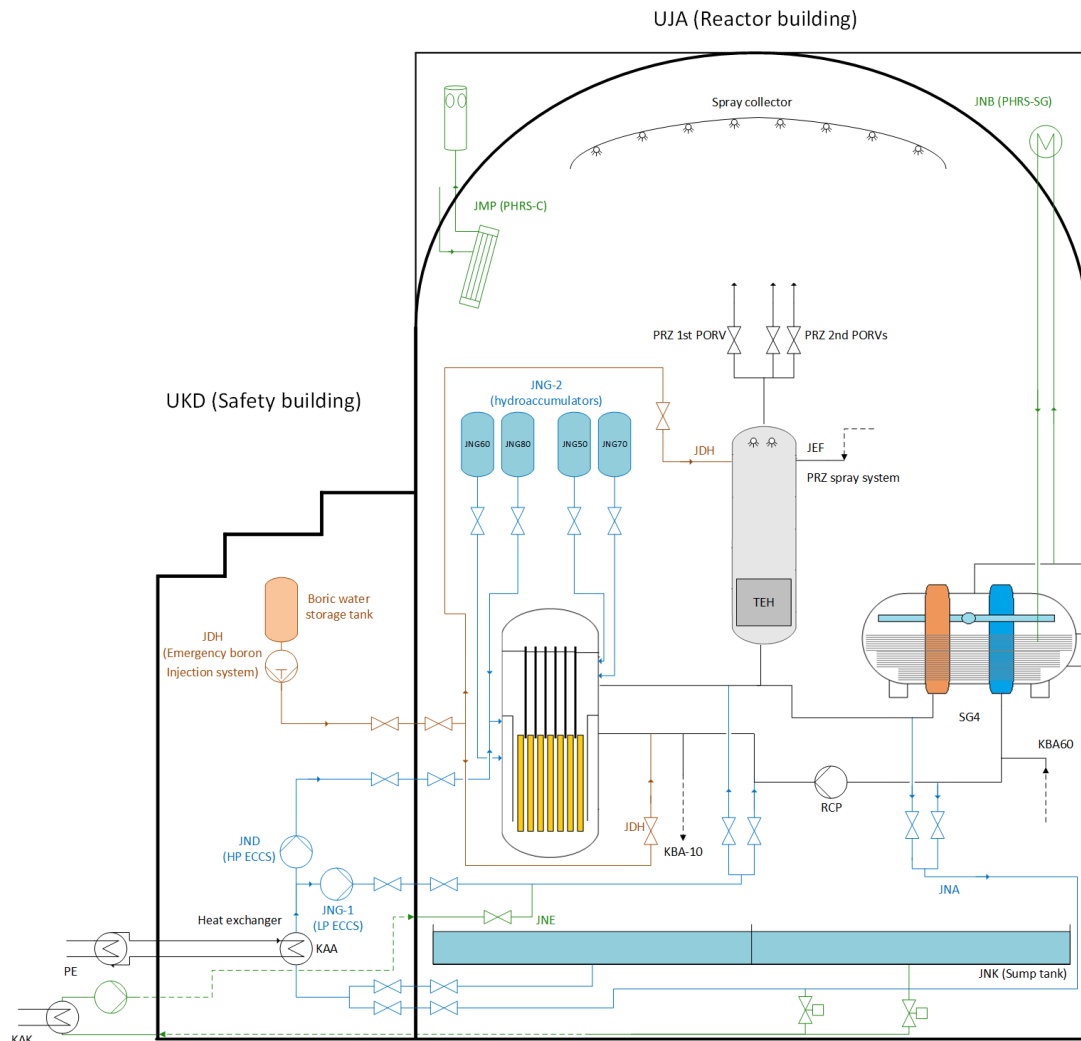


Figure 1: FH1 plant main systems (Zein, 2020)

In Figure 1, the reactor and the main components of primary loop 4 such as the pressurizer, steam generator and reactor coolant pump can be seen. In addition, the main safety systems are visible such as:

- Control rods in reactor
- Emergency core cooling systems with high- and low-pressure injections (JND & JNG-1) and hydroaccumulators (JNG-2)
- Residual heat removal system with recirculation (JNA & JNE)
- Emergency boron injection system (JDH)
- Chemical and volumetric control system (KBA)
- Pressurizer relief valves (PRZ PORVs)
- Steam generator (SG) and containment passive heat removal systems (JNB & JMP)
- Containment spray

Additionally, but not visible in Figure 1, the VVER-1200 plant design has a core catcher under the reactor to ensure that in core meltdown accidents, the corium cannot escape outside the containment. As this thesis studies the passive heat removal systems, these systems will be presented in more detail in the next subsection.

2.2 Passive heat removal systems

VVER-1200 as other generation III+ designs, have improved the safety aspects of nuclear power plants by incorporating an increasing amount of passive safety systems (World Nuclear Association, 2020). Such systems while not being inherently safe, increase the safety of a plant because their functioning does not rely on external factors. Passive safety systems are designed to utilise natural phenomena to achieve their function and thus to not need active intervention (Schulz, 2006). This removes possible operator errors and electrical power and signal failures (IAEA, 2009). However, as all

equipment and devices, passive safety systems are still prone to structural failures and therefore do not grant absolute reliability (IAEA, 1991).

The two new kind of safety system employed in the VVER-1200 are the SG and the containment PHRSs. The SG PHRS's objective is to remove heat from the steam generator by circulating the steam in the secondary side of the steam generators to heat exchangers in the PHRS tanks, condensing it and returning it as water to the steam generator. The containment PHRS's function in turn is to reduce and maintain the pressure inside the containment within design limits and to transfer heat to a heat sink, the PHRS water tank which itself is cooled by the atmosphere. (State Atomic Energy Corporation ROSATOM, 2013)

2.2.1 Steam generator passive heat removal system (JNB)

The SG PHRS (JNB) is a passive safety system that is designed to bring the plant to a controlled state and to maintain it in such state in accident scenarios. Furthermore, it is used to remove heat for extended periods of time from the primary circuit with the objective to transfer the plant to a safe state. The SG PHRS is a diverse system for the BRU-A, a system that lowers the pressure in the secondary side by using relief valves that release excess steam to the atmosphere. Thus, the JNB system offers another possible way to remove heat from the secondary side to the ultimate heat sink. This system is however not used in normal operating conditions nor in postulated accidents. (Fennovoima Oy, 2020a)

The SG PHRS functions by circulating heat in a closed circuit from the steam generators to the PHRS tanks. The tanks themselves are connected with pipes to the ultimate heat sink, the atmosphere, to allow the release of steam from the tanks. The JNB system is actuated by opening start-up valves which can function passively or using a power supply. After the opening of said valves, the whole system works passively. Steam that is created in the SGs

circulates naturally up the riser to the heat exchangers in the PHRS tanks in which the steam condenses back to water and flows through the downcomer back to the SGs. (Fennovoima Oy, 2020a)

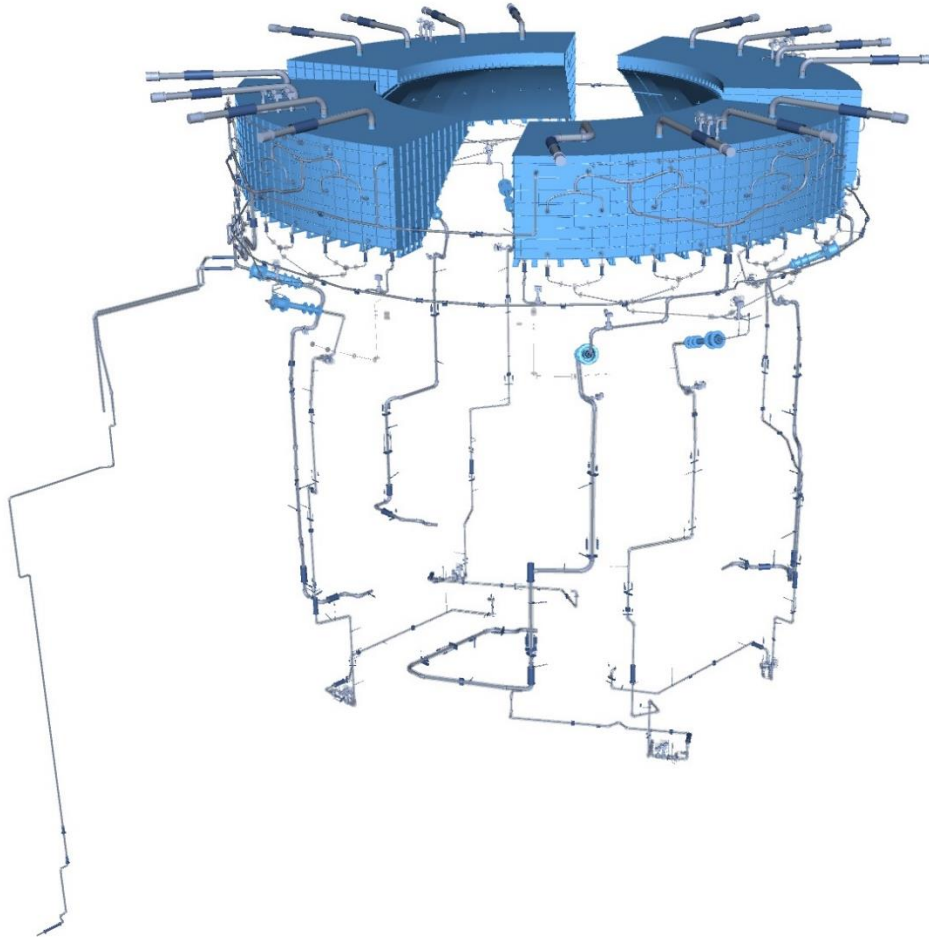


Figure 2: SG PHRS lines and the PHRS tanks (Fennovoima Oy, 2020a)

The JNB system consists of four identical subsystems: JNB10, JNB20, JNB30 and JNB40 (Fennovoima Oy, 2020a) which can be seen above in Figure 2. These subsystems are redundant, isolated functionally and separated physically. This is to increase reliability and safety of the plant by reducing the possibilities of common cause failures and to take in account single failure criterion (IAEA, 2000). A single subsystem consists of steam generator and its steam header connected to a riser pipeline. This line has two isolation

valves, on both in- and outside of the containment. On the outside of the containment, the line passes in to the PHRS tank and connects to the tube-type heat exchangers. From the heat exchangers, a condensate line goes back inside the containment and connects to the SG. Before the SG, there are two branches with two different sized start-up valves to allow the amount of heat transfer to be controlled. A schematic diagram of one subsystem is visible in Figure 3.

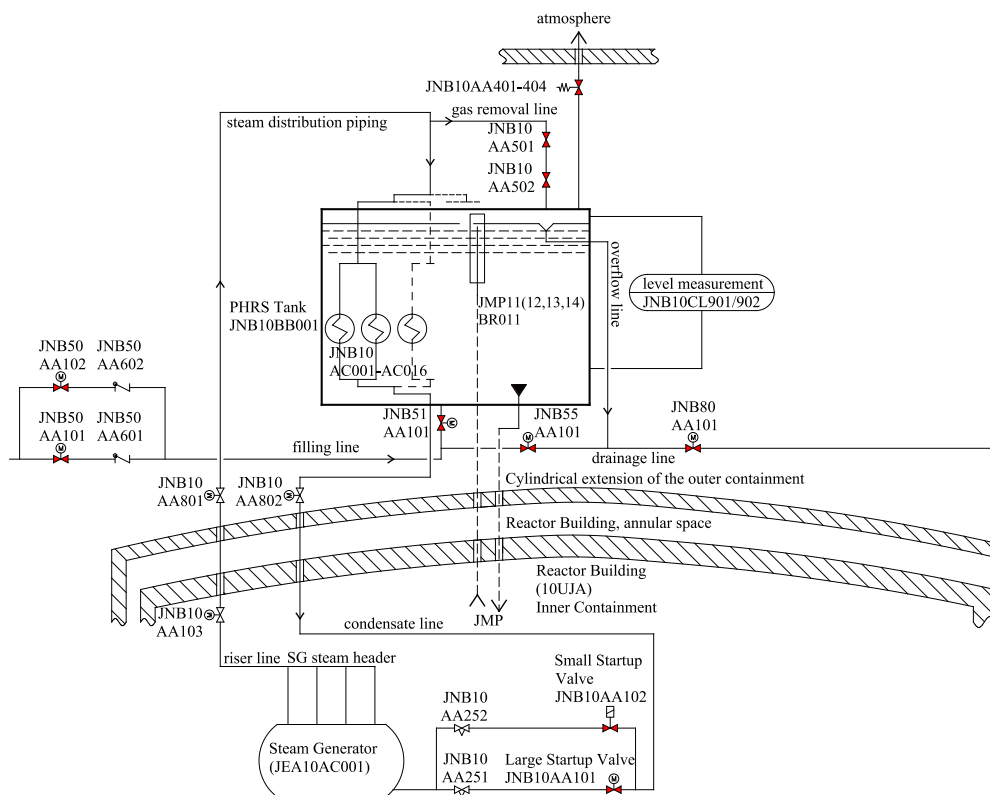


Figure 3: One subsystem of SG PHRS (Fennovoima Oy, 2020a)

During the operation of JNB, residual heat created in the reactor is transferred to the secondary side by the normal operation of steam generators. The JNB system is actuated by opening either of the start-up valves in the condensate line. The water in the secondary side turns to steam and through the JNB riser line goes up to the heat exchangers in the PHRS tank. In it the heat is transferred to the water in the tank which heats up and eventually

boils. The steam in the tank is released to the atmosphere via a passively opening valve. As the heat transfers to the tanks, the steam in the heat exchangers condenses to water and flows down through the condensate line back to the SGs by gravity. The returning water can then again vaporise in the SGs and start rising up to the heat exchangers. This way a closed loop is formed which removes heat effectively and passively using only natural circulation. (Fennovoima Oy, 2020a)

The SG PHRS is designed to remove decay heat from the primary circuit at an average rate of 30 °C/h and to cool it down to approximately 150 °C when using the small start-up valves. These are to be used during accident scenarios where the primary circuit is undamaged. The cooldown rate can go up to 44 °C/h when all four JNB subsystems are used. During loss of coolant accidents or primary-to-secondary circuit leaks, the large start-up valves can be opened which allow for greater heat removal capacities. With three active trains, these can go up to 150 MW. However, for such accidents the cooldown rates cannot be stated as they depend on the leak sizes and the pressures prevalent in the circuits. (Fennovoima Oy, 2020a)

The four PHRS tanks that are on top of the containment, are constructed of stainless steel and each house during normal operation 1072 m³ of water. When including the gas space in the tanks, the total volume is 1318 m³. The volume of the tanks has been designed to fulfil the 72-hours self-sufficiency criterion. This means that the amount of water in the tanks alone is enough to ensure decay heat removal from the reactor for 72 hours. (Fennovoima Oy, 2020a)

2.2.2 Containment passive heat removal system (JMP)

The containment passive heat removal system also known as JMP system is a safety system designed mainly for severe accident management. This means that the system is meant to keep the plant in a Severe Accident

Controlled State. The JMP system does that by ensuring the integrity of containment is not lost by an excess built-up of steam and a raise in temperature. During severe accidents such as core meltdown accidents, heat and vapor is continually released inside the containment. The CPHRS's function is to extract heat from the steam with heat exchangers and thus condense it and as a result reduce the pressure and the temperature inside the containment. (Fennovoima Oy, 2020b)

As the JMP system has this ability of heat removal from the containment, it is also of use in other accident scenarios than only during severe accidents (SA). In various design basis accidents (DBA) and design extension conditions (DEC) such as loss-of-coolant accidents and breaks of main steam line, release of steam takes place inside the containment for a prolonged time. In these situations, the CPHRS can work as an alternate way for heat removal if the primary system designed for it, the containment spray, fails. During normal operation, the JMP system has no function. (Fennovoima Oy, 2020b)

The containment passive heat removal system works by using heat exchanging surfaces inside the containment. Inside these sorts of radiators, water from the PHRS tanks, circulates to transfer the heat from the containment to the tanks outside of containment. The CPHRS, in contrary to the SG PHRS, is not a closed circuit. The inlet pipeline is connected to the bottom of the PHRS tanks from which water flows down to the heat exchangers, warms up and may turn in to steam. The heated water and steam rise from the heat exchangers through the outlet pipeline and reach the steam relief device, also known as a sparger. This is a cylindrical device that distributes the water and the steam inside the PHRS tank. (Fennovoima Oy, 2020b)

Similarly, to the SG PHRS, the CPHRS consists of four subsystems (JMP10-40) that are redundant, isolated and physically separated. Each of the subsystems consists of four identical trains connected to the same PHRS tank. A

single train has an inlet line with an isolation valve, four heat exchanging surfaces, outlet line with another isolation valve, steam distribution device and a condensate collector at the bottom of the heat exchangers with a connection to the floor drains. A single JMP subsystem is shown in Figure 4.

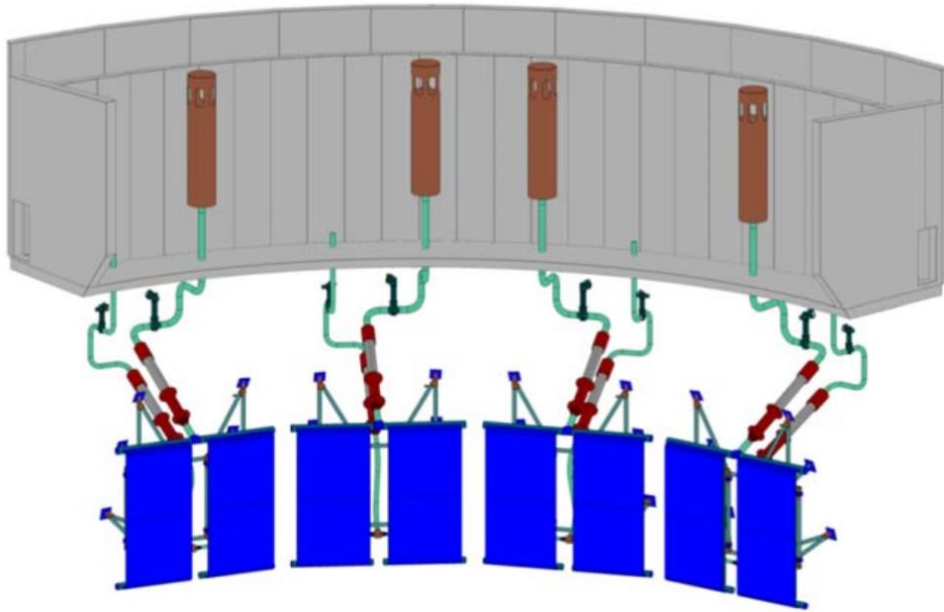


Figure 4: Containment PHRS subsystem (Fennovoima Oy, 2020b)

Being a passive safety system, the JMP functions with natural circulation only. The differences in water temperature and thus in water density, allows for the circulation of water between the heat exchangers and the PHRS tanks to take place. As steam is condensing inside the containment on the heat exchanging surfaces, the temperature of water inside the heat exchangers increases. This causes a temperature difference between the water in the condensers and the water in the PHRS tanks. Due to this temperature difference, the density also differs. This creates a buoyant force on the warmer water which pushes it up towards the PHRS tanks. As the resistances in the pipelines of the JMP system are low, the circulation of water from the heat exchangers to the tank starts already when a small difference of temperature exists. To supply more cooling water to the heat exchangers, cold water from

the bottom of the PHRS tanks flows down through the inlet pipeline to the heat exchangers to replace the water flowing up to the tanks.

After the CPHRS system has been in operation for a certain amount of time (depending on the prevailing conditions such as the containment temperature), the water at the JMP inlet line in the PHRS tanks reaches temperatures of around 65 °C. This causes the cooling water inside the heat exchangers to evaporate. The flow from the condensers to the PHRS tanks becomes a two-phase flow, a mixture of gas and liquid. As the heating of the tanks continue, the flow may also become a one-phase flow of only steam. At this point, the volume in the PHRS tanks is reducing and all the steam is released into the PHRS gas space and from there to the atmosphere. (Fennovoima Oy, 2020b)

A single JMP subsystem is able to provide 33% of the needed heat removal capacity in accident scenarios which corresponds to 5.32 MW. This means that 3 out of 4 subsystems are required to operate to maintain the temperature and pressure inside the containment below design levels. As with the SG PHRS, the CPHRS can operate 72 hours without any external power or water supply. (Fennovoima Oy, 2020b)

3 APROS SIMULATION SOFTWARE

To study passive safety systems and their functioning in various situations, the systems are modelled into computer simulation programs. Such programs model the nuclear power plant or a part of it. Fennovoima uses a simulation program called Apros Nuclear for safety analyses. This software has been developed by VTT and Fortum and is widely used in the modelling of nuclear power plants.

Apros is a multifunctional simulation software for modelling of various power plants and processes. It supports, full-scale modelling with vast model libraries and calculation algorithms. With these, complex industrial processes and power plants such as nuclear power plants can be modelled accurately. The nuclear models in Apros combines the neutronics of the reactor core with the thermal-hydraulics of the process components. In addition, the electrical system and the automation can be included to have a full model of the plant.

3.1 Neutronics

Apros has four options for reactor neutronics models. Point kinetics model, one-dimensional neutronics model and two different three-dimensional neutronics models. The 1D and the 3D neutronics models are both based on the two-group neutron diffusion theory in homogenised nodes (Fortum & VTT). Neutron diffusion theory allows the prediction of the neutron distribution in the reactor at different times by taking in account the different interactions the neutrons realise with different environments in the core. These interactions are approximated such that the neutrons undergo a diffusion in the core. This means that the neutrons distribute from a higher concentration to a lower one. To find out this neutron distribution, diffusion equations are

solved. The equations are based on the rate of change of neutron density. (Lamarsh & Baratta, 2001).

The two-group diffusion equations used in Apros as presented in (Puska, Rintala, Kurki, & Leskinen, 2015) are

$$\frac{\partial}{\partial t} \frac{1}{v_1} \phi_1 - \nabla \cdot D_1 \nabla \phi_1 + \Sigma_{b_1} \phi_1 = (1 - \beta) S_f + \sum_j \lambda_j C_j \quad (1)$$

$$\frac{\partial}{\partial t} \frac{1}{v_2} \phi_2 - \nabla \cdot D_2 \nabla \phi_2 + \Sigma_{b_2} \phi_2 = \Sigma_{12} \phi_1 \quad (2)$$

$$S_f = v \Sigma_{f_1} \phi_1 + v \Sigma_{f_2} \phi_2, \quad (3)$$

where

v_1 and v_2 are the fast and thermal neutron velocities

D_1 and D_2 are the fast and thermal neutron diffusion coefficients

ϕ_1 and ϕ_2 are the fast and thermal neutron fluxes

Σ_{b_1} and Σ_{b_2} are the fast and thermal neutron sums of absorption cross sections and absorption coefficients for control rods and soluble poison. The first term also takes in account the removal cross-section that a neutron goes from fast to thermal.

β is the total fraction of delayed neutrons

S_f is the neutron emission rate per cm³ from fission

λ_j is the decay constant of delayed neutron precursor group j

C_j is the concentration of the j^{th} delayed neutron precursor group

Σ_{12} is the removal cross-section for a neutron to go from fast to thermal

Σ_{f_1} and Σ_{f_2} are the fast and thermal neutron fission production cross-sections

The first equation (1) describes the change in fast neutron density by taking in account the emission, leakage and absorption rates. Similarly, the equation (2) describes the change in neutron density for thermal neutrons with the emission, leakage and absorption rates also taken into account. Finally, the third equation (3) defines the neutron emission rate per cm³ from fission as a sum of emission of fast and thermal neutrons.

Apros solves these equations by using methods such as mode decomposition and approximations of node boundaries. The calculations take into consideration six groups of delayed neutrons and in addition, the concentrations of burnable poisons such as iodine, xenon, promethium and samarium in the core are included. (Puska, Rintala, Kurki, & Leskinen, 2015)

3.2 Thermal hydraulics

For the thermal hydraulics part of the plant, Apros has five different accuracy levels to choose from. These levels differ from each other in the precision and the way they model the flow of fluids. The accuracy of the calculation that solves pressures, flows, enthalpies and temperatures of heat structures depends on the level used. The most accurate one, Flow model 6, models the fluids by calculating the afore mentioned parameters dynamically and constantly during simulation for two different fluids, e.g. for steam and water. This makes it precise and a good fit when simulating safety analyses. (Fortum & VTT)

3.2.1 Flow model 6

The two-fluid model used in the Flow model 6 is the most precise calculation of thermal hydraulics available in Apros. It is based on the conservation of mass, momentum and energy. These are defined separately for each phase

and various other phenomena such as friction and heat transfer are taken into account. The field equations used in Apros are the 3D two-fluid model field equations derived by area-averaging. There are six in total, three for each phase, and are presented in (Kurki, Ylijoki, & Leskinen, 2019). The equations for mass (4), momentum (5) and energy (6) for a phase are

$$\frac{\partial \alpha_k \rho_k}{\partial t} + \frac{\partial \alpha_k \rho_k u_k}{\partial z} = \Gamma_{i,k} \quad (4)$$

$$\frac{\partial \alpha_k \rho_k}{\partial t} + \frac{\partial \alpha_k \rho_k u_k^2}{\partial z} = -\frac{\partial p}{\partial z} + \Gamma_{i,k} u_{i,k} + \alpha_k \rho_k g + F_{w,k} + F_{i,k} \quad (5)$$

$$\begin{aligned} \frac{\partial \alpha_k \rho_k h_k}{\partial t} + \frac{\partial \alpha_k \rho_k h_k u_k}{\partial z} = \alpha_k \frac{\partial p}{\partial z} + \Gamma_{i,k} h_{i,k} + \\ Q_{i,k} + Q_{w,k} + F_{i,k} u_{i,k} + \alpha_k \rho_k u_k g, \end{aligned} \quad (6)$$

where

k subscript represents the phase of the fluid, i.e. liquid or gas

α_k is the volume fraction of the fluid of phase k

ρ_k is the density of the fluid of phase k

u_k is the velocity of the fluid of phase k

$\Gamma_{i,k}$ is the mass transfer rate between phases

$u_{i,k}$ is the velocity difference between phases

g is gravitational acceleration

$F_{w,k}$ is the friction between the wall and the fluid of phase k

$F_{i,k}$ is the friction between phases

h_k is the enthalpy of the fluid of phase k

$h_{i,k}$ is the enthalpy difference between phases

$Q_{i,k}$ is the heat transfer rate between phase

$Q_{w,k}$ is the heat transfer rate between the wall and the fluid of phase k

With the equations of mass, momentum and energy, the comportment of the fluids inside the process components can be calculated accurately. To achieve this, Apros carries out a discretization in which the state variables e.g. pressure and enthalpy are calculated in a node. In contrary, the flow variables are calculated at the border of the nodes. The properties of the fluids are obtained from a look-up table as a function of pressure and enthalpy. After the discretization, the parameters of pressures, velocities, volume fractions and enthalpies for each phase can be solved from the equations with an iterative process. (Fortum & VTT)

3.2.2 Convection heat transfer

In the Apros Flow model 6, four different correlation options exist to calculate the Nusselt number. The Nusselt number describes the proportion of convective and conductive heat transfer in a fluid. The four correlations available are the Dittus-Boelter equation, Sieder and Tate correlation, Gnielinski correlation and the Combined free and forced convection. These can be selected from the attribute Forced convection correlation of liquid (TH6_LIQ_FORCED_CONV_CORR) in the control module of the Flow model.

Conventionally, the option 1, Dittus-Boelter has been used in Apros model. This equation can be used to calculate the Nusselt number in a turbulent flow with forced convection. The Dittus-Boelter is a decent approximation when there are no large temperature differences between the fluid and the heat transferring surface. The equation relates the Nusselt number to Reynolds number and Prandtl number (Incropera, Dewitt, Bergman, & Lavine, 2006)

$$Nu = 0.023 Re^{\frac{4}{5}} Pr^{\frac{2}{5}}, \quad (7)$$

with the correlation valid for range

$$\left[\begin{array}{l} 0.6 \leq Pr \leq 160 \\ Re \geq 10\,000 \\ \frac{L}{d} \geq 10 \end{array} \right]$$

where L and d are the length and diameter of the pipe.

Option 2 is the Sieder and Tate correlation which is similar to the previous one but takes in account the viscosity of the liquid at bulk temperature (μ_B) and at the wall surface (μ_S). This makes the correlation more accurate but at the same time more complex. It is solved by an iterative process since the viscosity factor varies with the Nusselt number. The Sieder and Tate correlation from (Incropera, Dewitt, Bergman, & Lavine, 2006)

$$Nu = 0.027 Re^{\frac{4}{5}} Pr^{\frac{1}{3}} \left(\frac{\mu_B}{\mu_S} \right)^{0.14}, \quad (8)$$

with the correlation valid for range

$$\left[\begin{array}{l} 0.7 \leq Pr \leq 16\,700 \\ Re \geq 10\,000 \\ \frac{L}{d} \geq 10 \end{array} \right].$$

The third option is the Gnielinski correlation which is also a forced convection correlation. It however can be also used at lower Reynolds numbers down to 3 000 which at certain conditions is laminar. The Gnielinski correlation from (Incropera, Dewitt, Bergman, & Lavine, 2006)

$$Nu = \frac{\frac{f}{8} (Re - 1\,000) Pr}{1 + 12.7 \left(\frac{f}{8}\right)^{\frac{1}{2}} \left(Pr^{\frac{2}{3}} - 1\right)}, \quad (9)$$

where f is the Darcy friction factor

$$f = (0.79 \ln(Re) - 1.64)^{-2}. \quad (10)$$

The correlation is valid for the range

$$\left[\begin{array}{l} 0.5 \leq Pr \leq 2\,000 \\ 3\,000 \leq Re \leq 5\,000\,000 \end{array} \right].$$

Finally, the fourth option is the Combined free and forced convection. This option uses a correlation based on the Rayleigh number, which defines if the flow is laminar or turbulent in a free convection. A Rayleigh number smaller than approx. 10^9 is laminar and larger is turbulent. There are separate correlations that can be used depending if the flow is turbulent or laminar and also a single correlation that may be used for any Rayleigh number. This is the Churchill and Chu correlation (Incropera, Dewitt, Bergman, & Lavine, 2006) and shown below:

$$Nu = \left\{ 0.825 + \frac{0.387 Ra^{\frac{1}{6}}}{\left[1 + \left(\frac{0.492}{Pr}\right)^{\frac{9}{16}} \right]^{\frac{8}{27}}} \right\}^2. \quad (11)$$

The most appropriate correlation can be chosen from these four different correlations depending on the type of flow and convection present in the model. Currently the correlation change affects the whole model which is problematic. It is common for various flows and convection types to occur at different

places in the model which makes the choice of only one correlation difficult. This issue will be solved in the next major update for Apros (6.11), in which a different correlation can be set for specific parts of the model.

3.3 Containment

To simulate the movements of gasses inside the containment during transients and accidents, a separate model of the structure is needed. In the containment model, the volume of the containment is divided into sub volumes which are called nodes and the flow between the nodes are branches. The nodes are made of a gas region and may also include a “sump” which is any kind of liquid pool. The containment model in Apros uses the so-called lumped parameters (LP) method, in which the gas region of nodes is presumed to be a homogeneous mixture of non-condensable gases and water vapour which simplifies the calculations (Silde & Ylijoki, 2020a). In addition to the gas region and the sump, a node may also include fog droplets. These can be formed in the containment by condensation of water vapour or by injection through systems such as the containment spray. (Silde & Ylijoki, 2020b)

The containment model in Apros, similarly to the thermal hydraulics model of the process components, bases itself on the conservation of mass, momentum and energy. In the thermal hydraulics system of the containment, the three differential equations are used to solve the pressure, mass flow rate and temperature of a specific node. The equations for mass balance (7), momentum (8) and energy balance (9) reported by Silde & Ylijoki (2020b) are

$$\frac{\partial A\rho}{\partial t} + \frac{\partial A\rho w}{\partial z} = s_y \quad (12)$$

$$\frac{\partial A\rho w}{\partial t} + \frac{A\partial p}{\partial z} = s_y \quad (13)$$

$$\frac{\partial A\rho h_g}{\partial t} + \frac{\partial A\rho w h_g}{\partial z} = s_y, \quad (14)$$

where

A is the flow area of the node

ρ is the density of the gas mixture in the node

w is the velocity of the gas mixture in the node

p is the pressure of the node

h_g is the specific enthalpy of the gas mixture

s_y describes the sources of the mass, momentum and energy

Other specific safety systems and features may also be added to the containment model. These can be the spray system mentioned earlier, or for example, a condensation pool into which condensed steam will be collected. The transfer of heat between the gas region and one or multiple heat structure is calculated, and it is done with the Apros general heat conduction model. (Fortum & VTT)

4 HANHIKIVI-1 PLANT MODEL

Inside Apros, a model of the Hanhikivi-1 plant has been created. The Hanhikivi-1 Apros model has been in development since 2015 as a cooperation between Fennovoima and Fortum. The Apros model has all the main systems of a VVER-1200 V-522 modelled. These include the reactor, primary coolant loops, secondary circuits, containment, turbine, all main safety systems and their automation and electrical systems. (Peltokorpi & Hongisto, 2020)

4.1 Reactor

Nuclear power plant models in Apros are built using components from Apros library. The Apros library includes components for the nuclear part such as ready-made reactors, reactor channels, fuel rods and control rods. The FH1 reactor core is modelled in both 1D and 3D. The 3D model has 163 fuel assemblies with each in its own flow channel. Thus, 163 reactor channels are modelled and also 121 control rod assemblies. The core is divided into six sectors and each sector connected to the corresponding lower and upper plenum sectors. In the axial direction, the core is divided into 20 nodes. Between the reactor channels, cross flows are modelled in three separate levels. The data used in Apros for cross-sections has been calculated with CASMO-4E and the fuel burnups with HEXBU-3D. For LOCA analyses, a special core model has been developed, with fewer reactor channels but with denser axial nodalization. (Peltokorpi & Hongisto, 2020)

4.2 Primary side

For the process components, the Apros library has components such as pipes, valves and pumps among others. Using these components, the plant model can be built. For example, the four primary coolant loops of the plant are modelled using points, pipes and a reactor coolant pump. To demonstrate

this, a part of the primary loop 1 can be seen in Figure 5. The hot leg on the figure is the one above, coming from the upper plenum and going to the steam generator. The cold leg comes from the SG and is pumped by the reactor coolant pump back inside the reactor by the downcomer which's connection is visible at bottom left on the figure. (Fennovoima Oy, 2021)

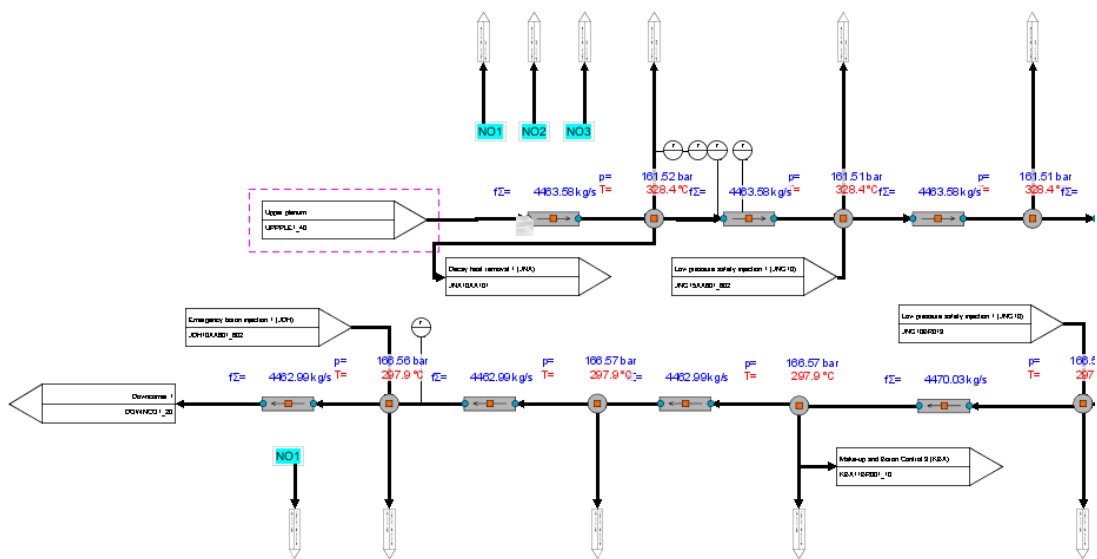


Figure 5: FH1 primary loop in Apros (Fennovoima Oy, 2021)

The flags connected to the components on the figure are connections. The larger flags are for major systems. The two connected on the left of the pipes are the connections to the reactor. Other larger flags are safety systems connections such as low-pressure or boron injection systems and decay heat removal systems. The small flags connected to all the points on this figure are heat transfer connections. They represent heat escaping from the primary circuit to the piping and the surroundings of the loop. The escaping heat is modelled with heat structure components.

4.3 Secondary side

For the steam generator, a specific component in Apros library models the horizontal SGs of a VVER. Its heat losses to the secondary side and the containment are also modelled using the heat structure components. The circular grey SG component is visible on the left in Figure 6. Connected to the SG are the inlet and outlet of the primary loop connections and the main and emergency feedwater lines. From the steam generator, the steam line takes the steam out of the reactor building through the containment isolation valves and towards the turbine. The containment isolation valves are the valves in green and the flag on the right of the figure represents the connection towards the turbine. The flag on top of the SG is the connection to the SG passive heat removal system and the four valves on the middle are the two SG pilot-operated relief-valves (PORV) and two BRU-A valves which can lower the pressure in the secondary side by releasing steam to the atmosphere.

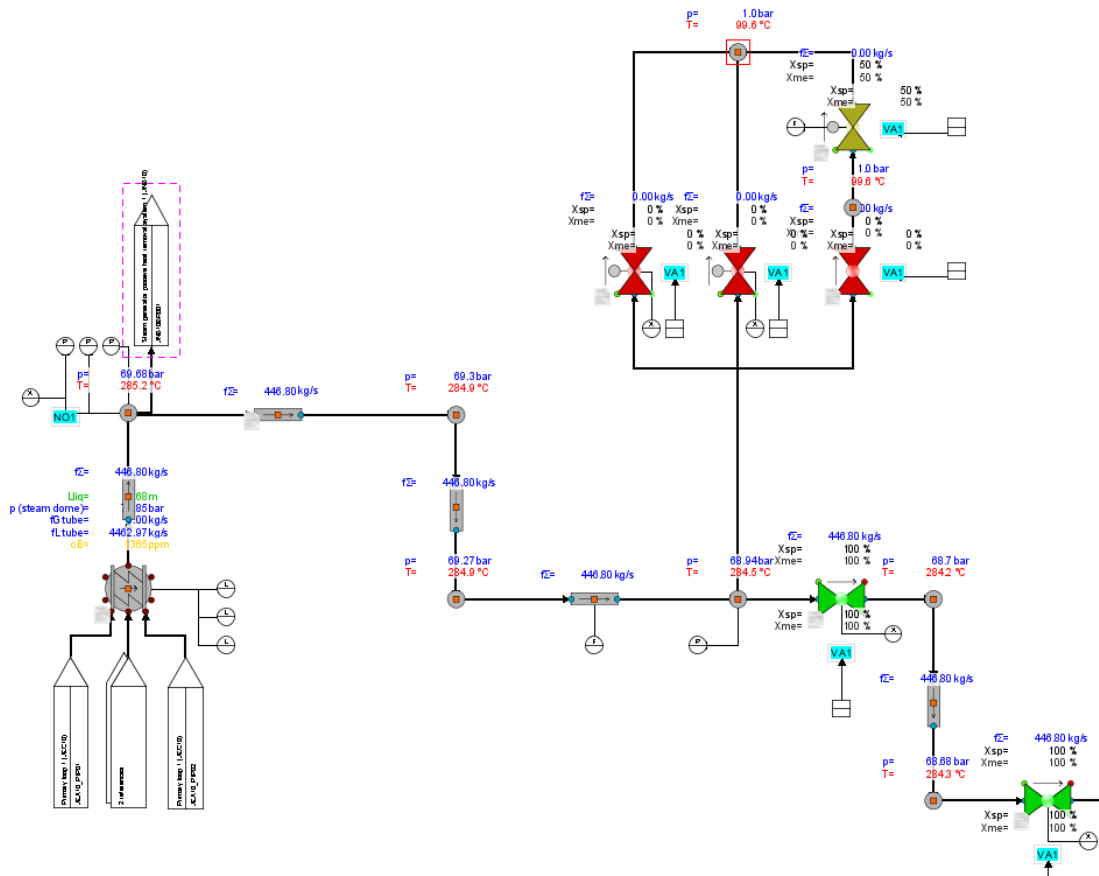


Figure 6: SG1 and steam line (Fennovoima Oy, 2021)

4.4 Containment

The containment is modelled with a large number of nodes connected between each other. These nodes model a certain volume of the inside of the containment. The nodes are connected with branches to simulate the gasses inside the volumes transferring between each other. To the nodes a sump component is connected, which keeps track of the liquid water present in the node. The source of this water may be condensation or from external sources. The sump component is then connected by a branch to a different node's branches or sumps to simulate the water flowing or falling to different areas of the containment. In addition, a heat structure component may be connected to the nodes to model the transfer of heat inside the containment to

the walls and other structures such as condensers. In Figure 7, two nodes (grey squares) can be seen each connected to sumps (blue). The two flags below the red line at the bottom are connections from the CPHRS system.

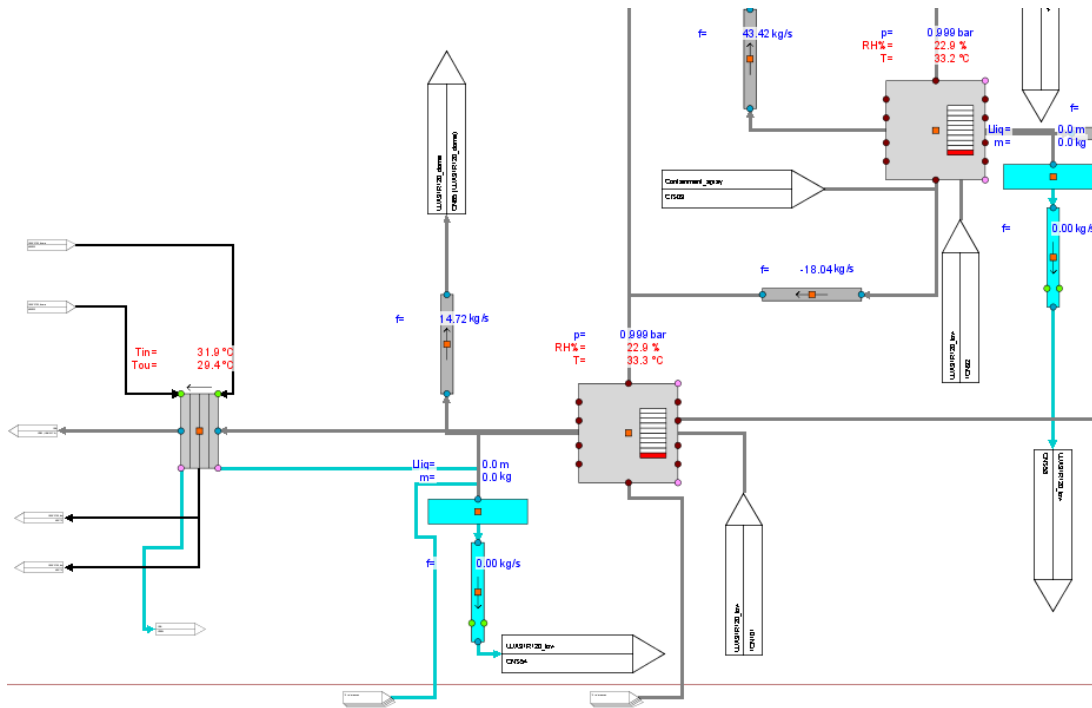


Figure 7: Part of FH1 containment model

4.5 Passive heat removal systems

The passive heat removal safety systems, the SG PHRS and the CPHRS, and the PHRS tank have been modelled in the plant model completely by using reference plant data. As the objective of this thesis is the V&V of the passive heat removal systems of the FH1 Apros model, the modelling of these two systems is described more precisely in the following subsections.

4.5.1 Steam generator passive heat removal system

The JNB system is modelled in Apros with four identical subsystems. A subsystem is connected to the point above the SG on the steam line as can be seen in Figure 6. To this point, the SG PHRS pipeline is connected. The circuit

model is made up of pipes, points and valves and it circulates through the PHRS tank. A JNB subsystem is presented in Figure 8. On it, one can see the riser line at the top and the condensate line at the bottom with each's two containment isolation valves. The condensate line has in addition two sets of two valves inside the containment. The bottom two are starting valves that are opened to start the system. The top two are control valves with which the total flow capacity is adjusted by modifying the pressure loss parameter. The condensate line is connected by a flag to a node which represents the water condensed in the heat exchangers returning to the steam generator. (Fennovoima Oy, 2021)

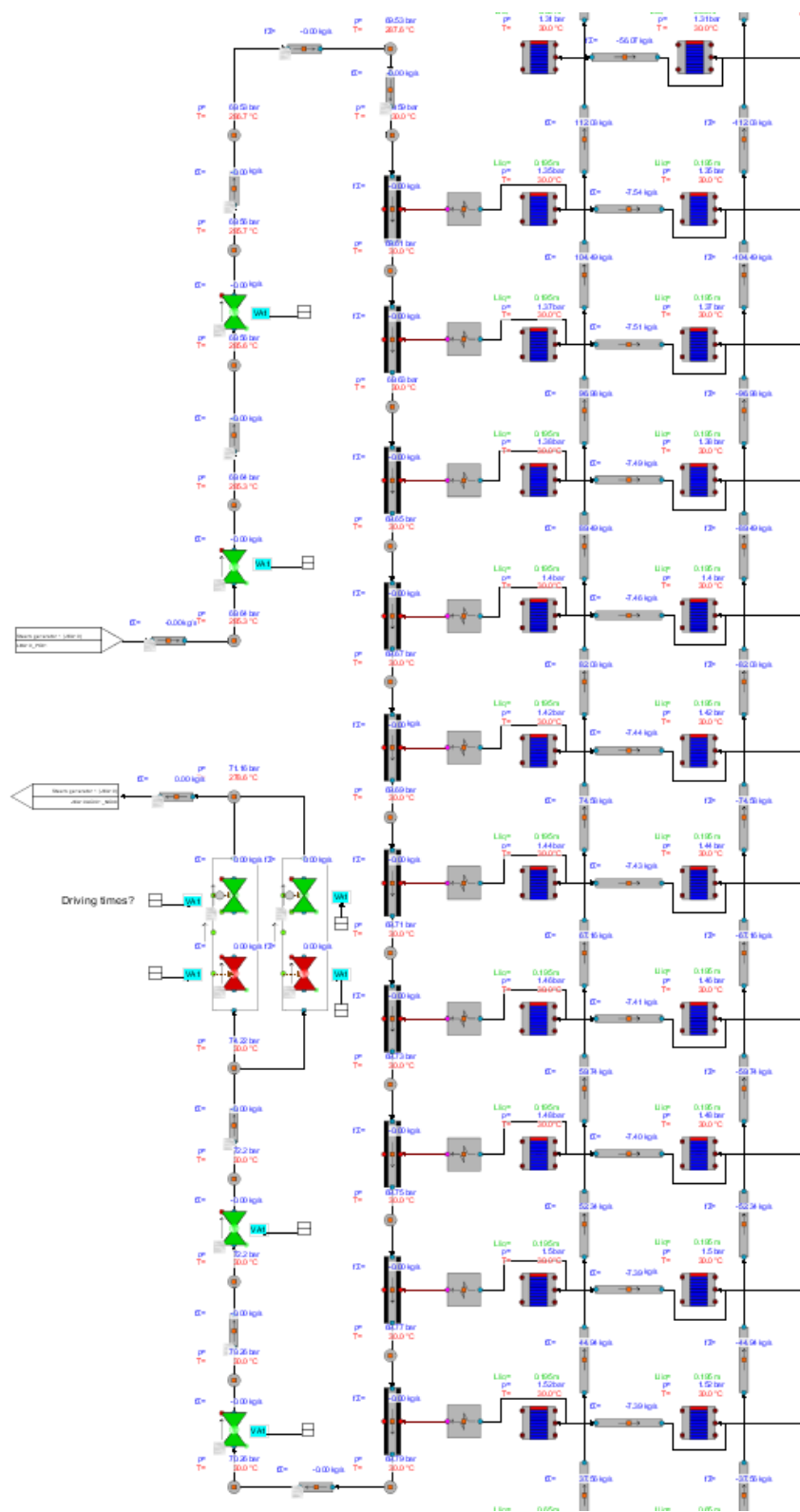


Figure 8: JNB subsystem (Fennovoima Oy, 2021)

The heat exchangers located between the riser and the condensate lines are modelled using a component called HEAT_PIPE. The 16 heat exchangers that would be present in the actual plant are simulated in Apros with 10 of these HEAT_PIPE components. The transfer of heat is modelled by connecting the HEAT_PIPE components to heat transfer components which are in turn connected to nodes. According to the documentation, the heat transfer capacity has been set to match the real-world capacity of the heat exchangers by varying the pressure losses of valves and pipes in the system. The capacity of the system in the model will be studied in the V&V section. (Fennovoima Oy, 2021)

A PHRS tank of one subsystem in the model consist of two rows of 19 nodes connected to each other. A single node represents a certain volume of water or air in the tank. During normal conditions, when the tank is at its nominal level, 34 bottom nodes represent the water volume and four nodes at the top the air volume in the tank. To the air nodes at the top, a pipe and a point is attached and depicts the connection to the atmosphere. In Figure 9 below, the SG PHRS is on the left and the 38 nodes in two columns next to it, are the PHRS tank. At the bottom of the PHRS tank, are the connections to and from the containment PHRS.

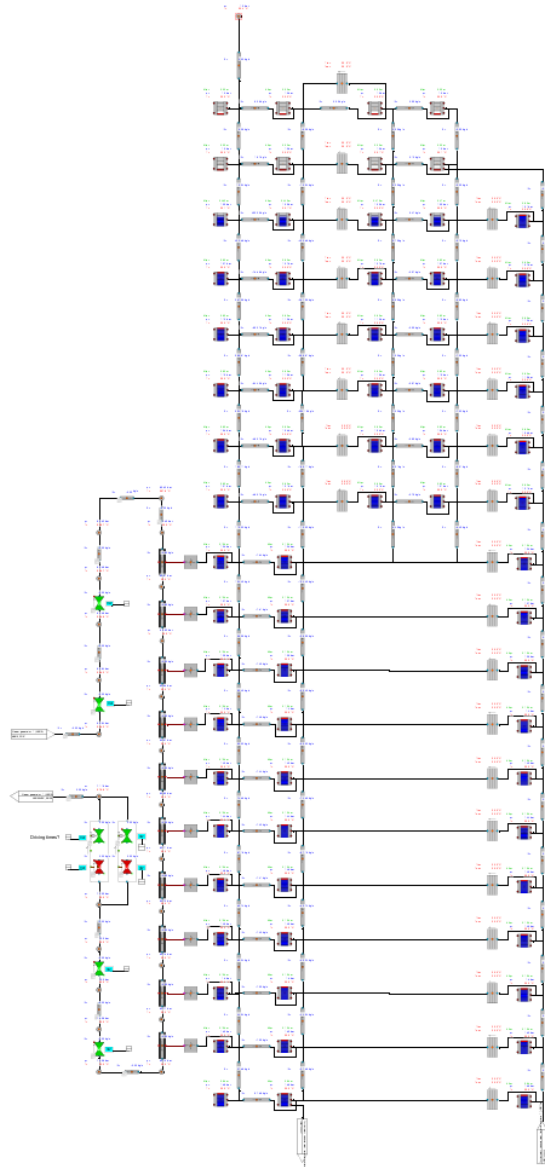


Figure 9: JNB system, PHRS tank and outlet line of JMP system

4.5.2 Containment passive heat removal system

The containment PHRS is modelled with four identical trains in Apros. The inlet line of the CPHRS connects to the bottom of the PHRS tank as can be seen in Figure 9. This allows for water to flow from the tanks through the inlet line to the heat exchangers/condensers. The heat exchangers of the JMP system are modelled using 10 vertical PIPE and 12 HEAT_STRUCTURE_X

components connected to the line where water from tanks flow (see Figure 10). The heat structure components are connected to the containment model nodes and sumps to simulate the heat transferring between the inside of the containment and the JMP system. From the heat exchangers, the water and steam that flows upwards towards the tanks is connected via a flag to the outlet line of the CPHRS (flag at the top in Figure 10) also known as the riser.

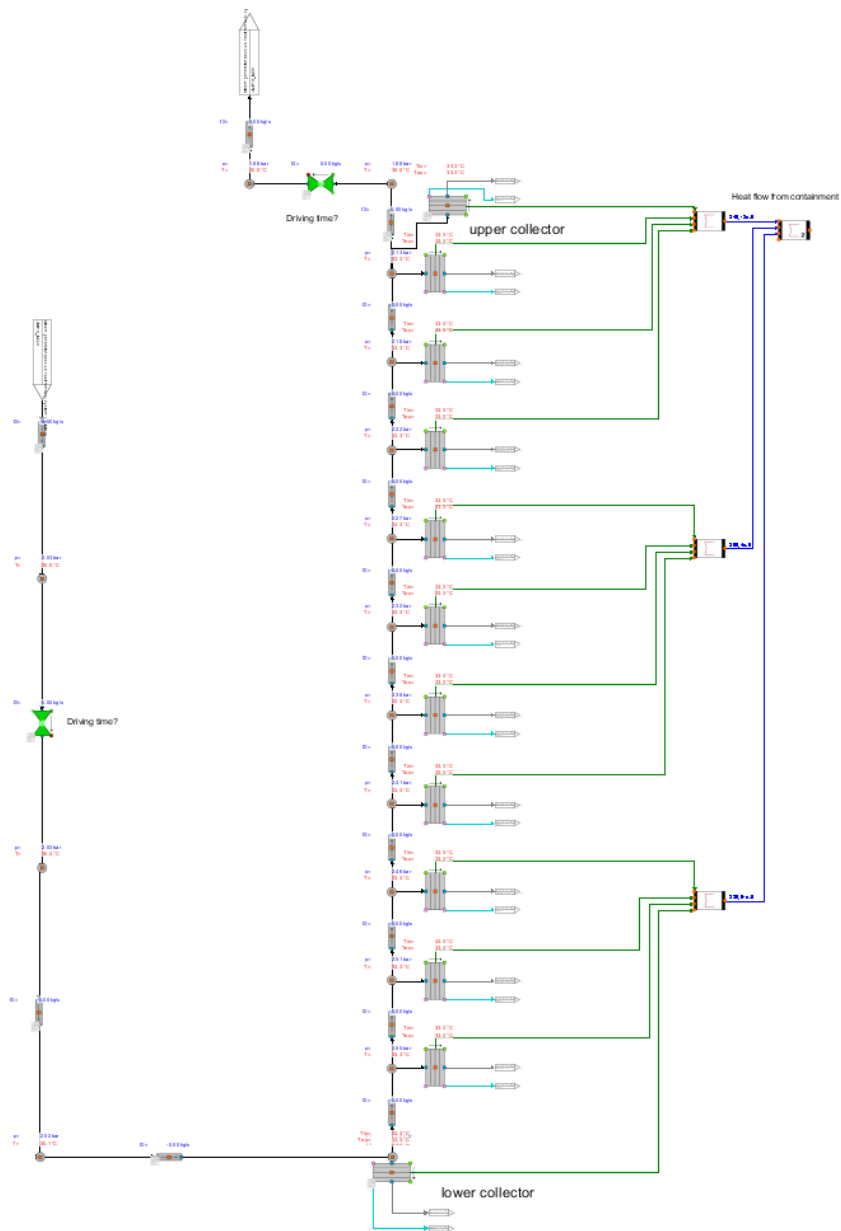


Figure 10: Containment PHRS

This outlet line is modelled using 17 nodes on rightmost side of the diagram in Figure 9. The 11 bottom nodes of the outlet line are connected to the PHRS tanks to simulate heat transferring through the pipeline to the water. The 6 top nodes of the outlet line are connected to the steam relief device to simulate the water and steam releasing from the outlet line to the water inside the sparger. This device is modelled using 16 nodes between the PHRS tank and the outlet line. Similarly, to the PHRS tank nodes, the four top nodes of the steam relief device are air nodes to model the air gap in the tanks.

At the start of this study, it was known that the JMP model had a modelling inaccuracy. In the system description, it is stated that the outlet line inside the sparger has a 50 mm hole. This hole is below the surface of water and it allows for liquid water to circulate out of the riser inside the sparger. The natural circulation occurs when a temperature and thus density difference takes place between the water in the system compared to the water in the PHRS tank.

In the current Apros model, this hole is not modelled and thus the only way for water to exit the sparger is through the larger holes at the top of the device. The holes are above water level and therefore a significantly greater temperature increase and thermal expansion is needed in the whole riser until the water is expelled from the outlet line via these holes at the top of the steam relief device. As the 50 mm hole allows for the water circulation in the sparger to take place substantially faster than without it, it has a considerable effect on the whole operation and heat transfer of the system. For this reason, the model is updated with this hole and this study uses the updated model to perform calculations.

5 VERIFICATION AND VALIDATION OF COMPUTER SIMULATION MODELS

The use of many computer simulation models assumes that the model has been constructed correctly and that it represents its real-world counterpart with only minor discrepancies. While simulation is an approximation of these real-world systems, the model and the information gathered from the model cannot be trusted unless it is proven that the simulation has the needed precision for the application. For this reason, when building simulation models, it is of utmost importance to confirm that the simulation has indeed been done accurately. This is demonstrated by a process called verification and validation (V&V). (Thacker et al., 2004)

5.1 Background

The verification and validation of computer simulation models has been a concern since the early days of digital computers in the 1950's (Sargent & Balci, 2017). Developers created simulation models and were testing these models to see if they functioned correctly. However, as Sargent and Balci state in "History of Verification and Validation of Simulation Models", in these early days of simulation, the V&V of these models was rarely explained and there was no common terminology for the process. Authors used the terms verification and validation interchangeably, Sargent and Balci note. Moreover, there was no accepted methodology to conduct a V&V and as the creation of complex models took a considerable amount of time and energy, the process of V&V was in some cases completely neglected.

In the late 1960's, the first articles that focused on the methods of V&V appeared. For example, Naylor and Finger in 1967 studied various validation techniques in their article, "Verification of Computer Simulation Models". In it the authors present a "*multistage validation*" procedure based on the

philosophy of science. These are rationalism, empiricism and positive economics. In the context of validation these mean respectively that the model needs to be developed logically and correctly, the assumptions of the model need to be empirically valid and that the outcomes of the model are correct while not being concerned with the assumptions or structure. Naylor and Finger state in their article that all these steps are required to be performed to achieve a high-quality validation of a simulation model.

Heading onto the 70's and 80's, the research and development of V&V skyrocketed, as stated by Sargent and Balci (2017). The importance and necessity of well-conducted V&V was recognized, which prompted plenty of studies and articles. This led to standardized definitions and accepted processes and methods for conducting V&V (Sargent & Balci, 2017). While the research on V&V has continued, the methods are mostly similar to those presented in (Sargent, 1988). These methods are used extensively. Some of them will be explained in subsection 5.3.

5.2 Definition

As stated earlier, model V&V is a process whose objective is to increase confidence in a simulation model by confirming that a numerical simulation model is accurately built and that it corresponds to the real-world (MITRE Corporation, 2013). V&V consists of verification and validation:

- **Verification** is the process of ensuring that the computer simulation model corresponds to the conceptual description and specifications of the system
- **Validation** is the process of ensuring that the simulation model is an accurate representation of the real-world system for the intended application of the model

This is also described in (Balci, 1997) where he clarifies that verification ensures that the model is built *right*, and validation ensures that the *right* model has been built. However, it is important to note that model verification and model validation are not entirely separate processes, and it is inevitable that parts of both processes may be conducted simultaneously (Winton, 2008).

5.3 Processes

To further explain the different entities and processes of V&V, R. Sargent created a simplified model development diagram in 1979, nowadays also known as Sargent diagram which can be seen in Figure 11. This diagram illustrates the different processes of model development. The problem entity is the real-world system, the conceptual model is the representation of the problem entity and the computerized model is the simulation model built with a computer program or code.

The diagram links the problem entity and the different models to each other. In the first place, for successful model development, accurate data is needed to create the models. To create a conceptual model, the real-world system needs to be studied and analyzed and on this basis a model can be made. To bring this conceptual model to a computer, the model needs to be implemented and programmed inside a software or code. To link the computerized model to the problem entity, experimentation needs to be done to ensure that the implementation has been successful and that the model indeed is representation of the real-world system.

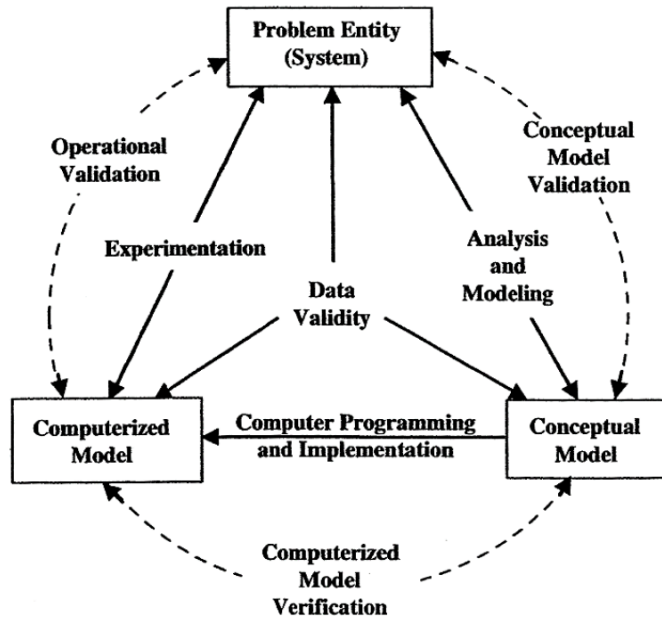


Figure 11: Simplified model development process (Sargent diagram)
(Sargent, 2020)

The V&V process then determines if the various steps of model development have been conducted correctly. To ensure that the assumptions and the representation of the problem entity used to create a conceptual model is precise, a conceptual model validation is done. Next the computerized model verification indicates whether or not the computer simulation model has been constructed correctly based on the conceptual model. Finally, the operational validation process reviews that the computerized model functions as expected, and its output is in line with the problem entity and its data.

5.3.1 Conceptual model validation

The validation of the conceptual model sometimes also referred as confirmation deals with ensuring that the suppositions and theories used to make the conceptual model are accurate to the needed precision (Sargent, 2015). In addition, the correctness of the depiction and structure of the model compared to the real-world system are studied. When creating a conceptual

model of a complex system, some simplifications are needed to build an efficiently working model. These simplifications are, however, done considering the accuracy required for the application of the model. (Carson, 2002)

Conceptual model validation methods are several with the most commonly used being face validity. The face validity technique means that potential users of the model and other experienced individuals of the system being modelled are incorporated to the development process of the model. These experts evaluate if the conceptual model is a reasonable representation of the real-world system by checking its fundamentals and functioning and giving constant feedback on needed changes. This contributes to better face validity and confidence as knowledgeable parties have been involved in its making. (Winton, 2008)

5.3.2 Computerized model verification

The verification of the computerized model refers to checking if the conceptual model has been correctly implemented to the chosen computer simulation program or code. During the development phase, a simulation model is constructed based on the conceptual model inside a software. All the components of the system being modelled are implemented considering the simplifications done during the development of conceptual model. However, as with all software development, errors and bugs may have occurred during the development of the simulation model. For this reason, a verification of the computerized simulation model is done. (Sargent, 2011)

This verification process is conducted through the computer program that the simulation model is built in. There are several methods to do model verification. One method is examining and meticulously checking all the components and their specifications that they match to the conceptual model specifications. This is important as typing errors are common and could lead to inaccurate results. Other verification methods can be such as model testing

with various input data, checking if model output seems correct and observing the behaviour of the model during simulation. (Tsang, 1990)

5.3.3 Operational validation

The operational validation, also sometimes referred simply as validation of simulation model, is the validation process that determines if the output and results of the simulation model have the precision needed for the application of the model. Erroneous outputs may be caused by flaws that took place during the conceptual modelling or during the implementation of the computerized model. It is also possible that the data used for modelling is invalid or bugs may be present in the simulation code. To ensure that the model is correct, deep testing and evaluation is carried out. (Sargent, 2020)

As stated at the beginning of this chapter, simulation models are only approximations of real-world systems and thus will always have certain inaccuracies. With operational validation, the accuracy of the model can be quantified. The most common method is to conduct statistical and graphical comparisons between the model outputs and results and the data of the real-world system if such is available. The model data can also be compared to the data of another model that has been verified and validated. When performing the comparisons of data, it is better to have data from various situations to study the system and model behaviour more thoroughly. (Sargent, 2020)

6 RESEARCH METHODS

6.1 Verification methodology

Returning to the Sargent diagram (Figure 11) presented in the previous chapter, in our study the problem entity corresponds to the passive heat removal systems of steam generator and containment of the FH1 NPP. The conceptual model represents the theoretical model and functioning of the passive heat removal systems and finally the computerized model is the simulation models of the passive heat removal systems built in Apros.

In order to conduct a model V&V, generally three different processes are done. The validation of the conceptual model, the verification of the computerized model and the operational validation of the simulation model. The FH1 plant model has been developed by experts from Fennovoima and Fortum based on information received from the Supplier. As such it could be said that the conceptual model already had a high face validity. Nonetheless, as the models of the PHRSs were built several years ago with less information than available today, it was deemed that both the conceptual validation and computerized verification for these systems were necessary.

As the two processes of conceptual validation and the verification of the computerized model are closely related, they were done and reported jointly. This is due to the overlapping nature of these processes and the methods to carry out these and as such they will be performed together. In addition, to simplify the reporting and terminology for the results section the process of conceptual validation and the verification of the computerized model is from here on referred simply as verification (as opposed to the operational validation referred simply as validation).

The verification was done by checking and comparing the systems and the components of the model in question with the specifications of these components described in the design documentation received from the Supplier. With this, it was ensured that the model is built right and that the systems are modelled correctly and correspond to the real-world system. In addition, preliminary calculations were done with the model in question to test the simulation and the changes made.

6.2 Validation calculations

To conduct the operational validation of the passive heat removal systems models, different calculations were done. For the SG PHRS and the CPHRS, these match to the commissioning tests conducted at LAES-II reference plant in 2017. In these tests the functioning and the heat removal capacity of the system was assessed by completing 3 different tests for the SG PHRS train 1 and one test for the CPHRS train 1. The plant was in the following state:

- No fuel in reactor (hot-functional tests state)
- All 4 reactor coolant pumps operating and producing approx. 20 MWt
- Primary circuit temperature is 285 °C
- Primary circuit is fully insulated with heat losses of approx. 2 MWt
- Primary circuit pressure is 16.2 MPa
- Secondary circuit pressure is 6.65 MPa
- PHRS tank temperatures were 25 °C for the tanks 1, 3 and 4 and 65 °C for tank 2

To carry out the calculations, the Apros model is modified and run to a similar state. The reactor was shut down and the decay heat was set to zero. The turbine was excluded as it did not have a function in these cases. The heat created by the RCPs was adjusted from the model default value of approx. 22 MWt to value stated in the report (Geraghty et al., 2017) of 20 MWt by modifying the hydraulic torque curves of the pumps. The primary circuit pressure

was adjusted by PRZ heaters and the secondary pressure and level with bypass line of feedwater system and the BRU-A release valves.

With the plant in a similar state to the reference plant during the commissioning tests, the calculations were started. The calculations were done as closely as possible to the commissioning tests described in the Supplier's report (AO Rosenergoatom, 2017a). However, because the document does not include all information on the plant state nor the exact values of all parameters before and during the tests, some had to be estimated.

The JNB system was tested with three runs on the train 1. First the bypass line of feedwater system and the BRU-A release valves were closed. Then the small starting valve (solenoid valve) was opened which initiated the operation of the system through the small valve. This was kept open for 18 minutes and then closed. The second test was through the large starting valve (motor operated valve) with no hindrances to flow. This was to test the maximum capacity of the system through the large valve and was run for 17 minutes. The last test was also through the large valve with objective to lower the flow and heat transfer to match the design capacity of the system. The flow was decreased at LAES-II by closing of manual control valve, in Apros this was done by varying the losses of the system components. This last test was run for 7 minutes.

For the CPHRS system, the calculations were conducted as reported in Supplier's document (AO Rosenergoatom, 2017b) on commissioning tests. During these tests, the train 1 of the JMP system was tested. To replicate the tests, the Apros model's containment temperature was heated up to a value of 56 °C. As the humidity in the containment was stated to be low, but no exact value for this was given, a sensitivity analysis was done by varying the amount of humidity. From this analysis, the humidity level that was deemed to be closest to the conditions at the reference plant was chosen to be studied

further. The tests were started by opening the isolation valves of the JMP system up- and downstream from the heat exchangers. The temperature difference between the heat exchanger inlet and outlet, the power of the JMP system and the mass flow through the system was tracked.

7 RESULTS

7.1 Steam generator passive heat removal system

7.1.1 Verification

During the verification process, it was noticed that the SG PHRS model had inaccuracies that needed to be fixed before validation could be started. The heat exchangers of the system were modelled using 10 HEAT_PIPE components as described in the subsection 4.5. When the total surface of these heat exchangers was calculated this resulted in 239.15 m². According to the report (JSC Atomproekt, 2020), the heat exchanging surface of a heat exchanger is 14.93 m² and with 16 heat exchangers, this equals to 238.88 m². However, these surfaces do not include the headers of the HE. The top and bottom headers also contribute to the heat transfer, and as such they must be included in the model to have accurate results. As the difference in surfaces between the model and the report is $239.15 \text{ m}^2 - 238.88 \text{ m}^2 = 0.27 \text{ m}^2$ apart, it confirms that the computerized model does not have the headers modelled.

The headers of the heat exchangers were modelled by a node which was connected to the heat pipes by a branch component at the top and bottom of the HEs. In addition, a heat structure component was connected to the new node and the other end to a node in the PHRS tank. This heat structure component models the heat transfer from the header to the water in the tank. The new components for one header added to the model can be seen on the Figure 12.

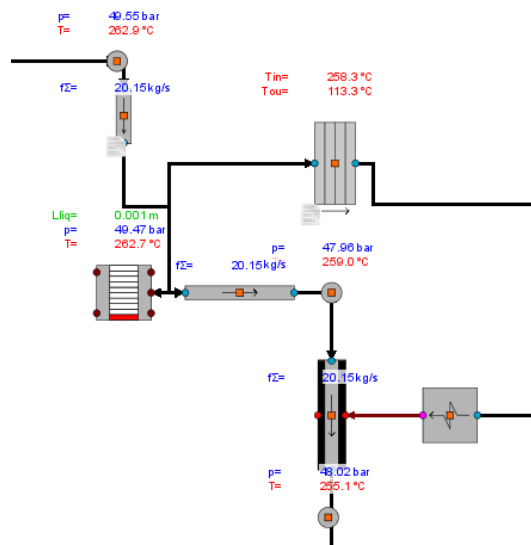


Figure 12: Top header of the HEs in the updated Apros model

Additionally, the nodes of the PHRS tank on the JNB diagram were modified. Several extra nodes were added to correct the volume-height curve to match the shape of the tank. Additionally, as newer, up to date information has been received on the exact positions of the systems in the PHRS tank, the height of the nodes was also adjusted. This was done in order to correct the JNB and JMP systems' position in the tanks.

With the model updated, the system was tested. As a result, from systematic testing, the condensate temperature in the condensate line below the heat exchangers was substantially higher compared to the results from the commissioning tests at the reference plant. Thus, the problem was in the heat transfer and more precisely the heat convection from the outer surface of the heat exchangers to the PHRS tank. To correct this, the convection heat transfer correlation needed to be changed.

Conventionally, the FH1 Apros model uses the Dittus-Boelter correlation (option 1 in Apros) for the whole plant (see section 3.2.2). This works well for forced convection calculations but as the heat transfer from the outer surface

of the JNB heat exchangers to the PHRS tank is free convection, it was not valid to be used in these PHRS validation specific calculations.

To identify the situation further, the Rayleigh number for the heat transfer from the outer surface of the heat exchanger to the PHRS tank was calculated. This was to find out if the flow is laminar or turbulent and therefore the correct convection heat transfer correlation to be used. This was done by creating a user-component in Apros that calculates the Rayleigh number using the following equation (15) taken from (Incropera, Dewitt, Bergman, & Lavine, 2006)

$$Ra = Gr Pr = \frac{g B (T_s - T_\infty)L^3}{\nu w}, \quad (15)$$

where

g is the gravitational acceleration

B is the thermal expansion coefficient

T_s and T_∞ are the temperatures at the surface and in the PHRS tank

L is the characteristic length of the geometry

ν is the kinematic viscosity

w is the velocity of the gas mixture in the node

The equation (15) is created in Apros as a user-component (see Figure 13). In Figure 14 the user-component is in use. It is connected through value transmitters to the outside surface of the heat exchangers and a node in the PHRS tank. The output of the component is given as a signal from the red dot.

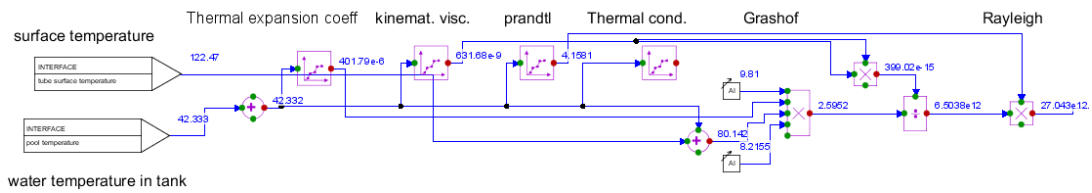


Figure 13: The created user-component inside Apros

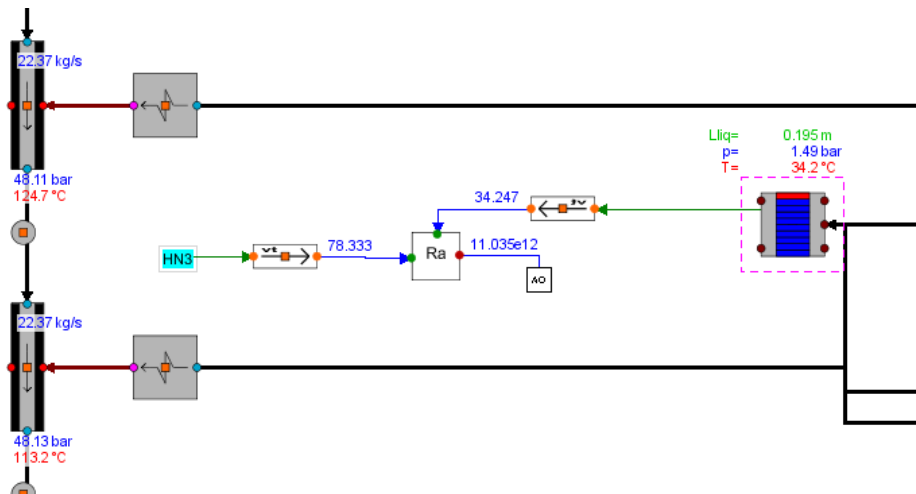


Figure 14: The user-component (Ra) added to the JNB diagram

Calculating the Rayleigh number gave a value in the range of 10^{12} for both the top and bottom part of the heat exchanger which means that the flow on the outer surface of the heat exchangers is turbulent. Thus, naturally the correlations for laminar flow such as the Gnielinski correlations cannot be used. To get the most accurate results for the PHRS heat transfer, the correlation was changed to Churchill and Chu correlation (option 4) which is valid for free and forced convection and for both laminar and turbulent flows.

The change fixed the heat transfer inaccuracies in the JNB system while there were no noticeable variations to the flows and heat transfers in the rest of the plant. The differences in results for the two correlations are on the Table 1 for the train 1 of JNB system with small valve open and loss coefficients set to the default values.

Table 1: Results for preliminary test calculation with correlation options 1 and 4.

	Dittus-Boelter (option 1)	Churchill and Chu (option 4)
Mass flow (kg/s)	10.5	12.8
Heat flow (MWt)	22.4	29.8
Condensate temperature (°C)	119	53

As can be seen from Table 1, with option 4 active, the heat transfer is augmented. The free convection correlation allows for better transfer of heat from the heat surfaces to the PHRS tank. This is visible on the temperature of the condensate. With option 4 active, the JNB system is able to extract more heat from the water flowing through the heat exchangers.

The designed system capacity for one train is approx. 28 MWt with small valve and 52 MWt with large valve (Fennovoima Oy, 2020a). However, the results from the commissioning tests show that the maximum measured capacity for small valve was 25 MWt and 60 MWt for large valve. This difference was explained by Atomproekt engineers by the smaller valve having a higher friction than designed. Friction on the valve slows down the flow rate in the system and therefore reduces the heat transfer.

To match the heat and mass flows measured at reference plant to the values of Apros, the pressure losses of the control valves were adjusted. The exact losses of the JNB components are not yet known, and as such they were fine-tuned so that the mass flow through the system is as close as possible to the LAES-II measurements. The JNB mass flow with the small valve was higher in Apros than the value in the commissioning tests and thus the pressure loss of the control valve downstream the small solenoid valve was increased to 0.47. For the large valve, the pressure loss was decreased to 0.1 as the mass flow was in contrary initially lower than in the commissioning tests.

7.1.2 Validation

With the above modifications done, the validation calculations were started. The SG PHRS validation was done by completing three test runs with train 1 of JNB system: one with small valve and two with large valve. The tests were done imitating the commissioning tests at LAES-II (AO Rosenergoatom, 2017a) to allow for efficient benchmarking. A summary of the tests performed are in Table 2.

Table 2: Test runs for JNB system.

	Test 1	Test 2	Test 3
Valve opened	Small starting valve	Large starting valve	Large starting valve
Duration (min)	18	17	7
Valve position	100% open	100% open	70% open

To test the functioning of the JNB system, two parameters were tracked closely: primary circuit temperature and pressure in steam generator 1. These two parameters allow to examine, how effective the heat removal and pressure reduction has been. The temperature of PHRS tank was also plotted however, the size of the tank is different in FH1 and LAES-II. The volume of the FH1 tank is 1080 m³ and that of LAES-II is 550 m³. As the difference is almost twofold, direct comparison of temperature is pointless.

Data on the commissioning tests were available in the Supplier's report in the form of a graph and thus allowed for comparisons of data to be made. Other information such as JNB mass flow and power were simply listed in a table with only one value for each test run. The pressure in primary circuit was another potential parameter, but the changes to it during the tests were minor and the data available on it is of poor quality.

Test 1

To start the calculations, the initial conditions of the Apros model were brought as close as possible to the values of commissioning tests. In Table 3, the values of the three parameters are presented at the start of test run 1. The largest difference was in primary circuit temperature, which had a difference of 2.7 °C between Apros and LAES-II. This corresponds to a difference in temperature of only 0.96% and as such it was deemed to not affect the validation process significantly.

Table 3: Initial conditions for test 1, small valve.

	Apros	LAES-II
Primary circuit temperature (°C)	282.1	284.8
SG1 pressure (MPa)	6.65	6.64
PHRS tank 1 temperature (°C)	25.0	25.0

With the Apros model in a similar state to LAES-II, the first test run was started. The valves of the bypass line of the feedwater system were closed which ceased the flow of feedwater into the steam generator. Additionally, the BRU-A valves and the MSIVs were closed which in turn stopped the flow of steam out of the steam generator and its nearby lines to the atmosphere and to the turbine. These valve closures made sure that the steam generator was isolated and that the only way to remove the heat of the primary side brought to the secondary side was via the SG PHRS system.

The test run 1 was started with the opening of the small starting valve of the JNB system at 19:41:45. This started the flow of steam from the SG up to the heat exchangers. When the steam which was approx. 279 °C reached the header and the top of the HEs, it condensed. The condensate flowed down the HEs and kept cooling until it reached the bottom of HEs and was of temperature 50 °C. The mass flow through the system increased at the start to a

value of 10.1 kg/s but then stabilised to approx. 9.65 kg/s. Table 4 shows the results of test 1. The trend figures of test 1 are in Appendix 1.

Table 4: Results of test 1, small valve.

	Apros	LAES-II
Test duration (min)	18	18
Primary circuit temperature start (°C)	282.1	285.0
Primary circuit temperature end (°C)	278.0	278.0
SG1 pressure start (MPa)	6.65	6.64
SG1 pressure end (MPa)	6.14	5.94
PHRS tank 1 temperature start (°C)	25.0	25.0
PHRS tank 1 temperature end (°C)	28.8	27.5
Mass flow through JNB (kg/s)	9.65	9.65
JNB power (MWt)	24.8	24.7
Cooling rate (°C/h)	13.7	23.4

As can be seen from the table, the results are very similar and the differences in primary circuit temperature and SG pressure are minor. At the reference plant, for the same JNB mass flow and capacity, the real system with small valve reduced the temperature and pressure slightly more than what Apros predicts. This can be attributed to variation in real-world operation of the system. For example, the exact cooling rate of primary circuit when JNB system is operating with small valve can vary between tests significantly. This can already be seen in the report on the commissioning tests where the cooling rate of the trains varies between 14.6 °C/h and 23.4 °C/h.

Other possible factor that brings uncertainty to the results is the fact that there is no precise information on the location of the measurement devices at LAES-II. In the primary circuit, the temperature varies by about 2 °C

between the hot and cold legs. This difference can account for some of the variations in results. In Apros, the temperature is taken from the cold leg at the reactor inlet. In Figure 15, the primary circuit temperature during the test run 1 is shown for both Apros and LAES-II.

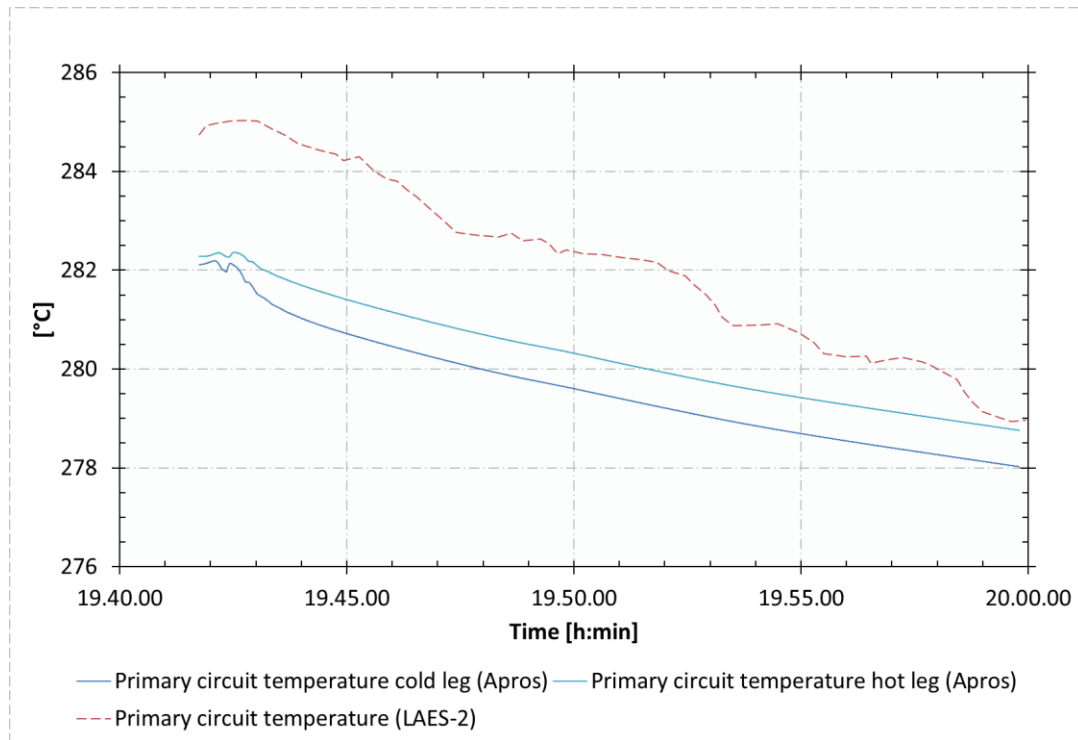


Figure 15: Primary circuit temperatures during test 1.

Regarding the PHRS tank temperature, the Apros one is higher. This should not be the case due to the tank size difference explained earlier. The explanation for this anomaly is that the temperature measurement location is unknown at the reference plant. For Apros the measurement location is node 28, which is the third node from the top that is connected to the Heat_pipe components. It is fair to say that the water in this node heats up quicker than where the measurement was made at LAES-II and thus the location is inaccurate. Nonetheless, as the tank sizes are different and therefore the temperatures are not comparable, it was decided to not change the measurement location.

Test 2

The second test run was using the large valve 100% open with no limitations to the flow. With this run, the maximum flow and capacity of the system was tested. Flow limitations at LAES-II were done with the manual control valve and in this run the valve was 100% open. With Apros to achieve similar system performance as measured at reference plant, the pressure loss of the control valve was modified to 0. In addition, the loss coefficients of several pipes and isolation valves were reduced to increase the mass flow through the system. As a result from these changes, a maximum JNB power of 59.8 MW was reached with average power during the test around 57.5 MW. Table 5 shows the results for test run 2.

Table 5: Results of test 2, large valve 100% open.

	Apros	LAES-II
Test duration (min)	18	17.8
Primary circuit temperature start (°C)	280.7	281.4
Primary circuit temperature end (°C)	262.3	266.2
SG1 pressure start (MPa)	6.46	6.40
SG1 pressure end (MPa)	4.76	4.60
PHRS tank 1 temperature start (°C)	28.7	27.9
PHRS tank 1 temperature end (°C)	38.5	44.7
Mass flow through JNB (kg/s)	24.5	24.1
JNB power (MWt)	57.5	59.6
Cooling rate (°C/h)	61.3	51.2

The results for test 2 are comparable with slight differences to the end values of primary circuit temperature and SG1 pressure. The reason for these

deviations can be again explained by the variations of the system during operation and from the uncertainty induced by the measurement locations. The size difference of the PHRS tank is also visible with the temperature of water at LAES-II heating considerably faster than in Apros.

The power of the JNB system, exceeded the design value of 50 MW. This was expected as at the reference plant, powers over the design thermal power were reached with full large valve capacity. Values close to 60 MW were reached in both Apros and at LAES-II. As to the cooling rate of primary circuit, for Apros it was calculated to be 61.3 °C/h when using the cold leg temperature and 53.3 °C/h when using the hot leg temperature. This difference is mostly caused by the start-up of JNB system in the beginning of the run. After this, the cooling rate in both legs is identical. Comparing the cooling rate with LAES-II, the results are very similar, and the slope of the curves match closely (see Figure 16). The cooling rate in Apros and LAES-II are close to the design maximum cooling rate of 60 °C/h and as such the modelling seems to be accurate. The rest of the trend figures for test 2 are in Appendix 1.

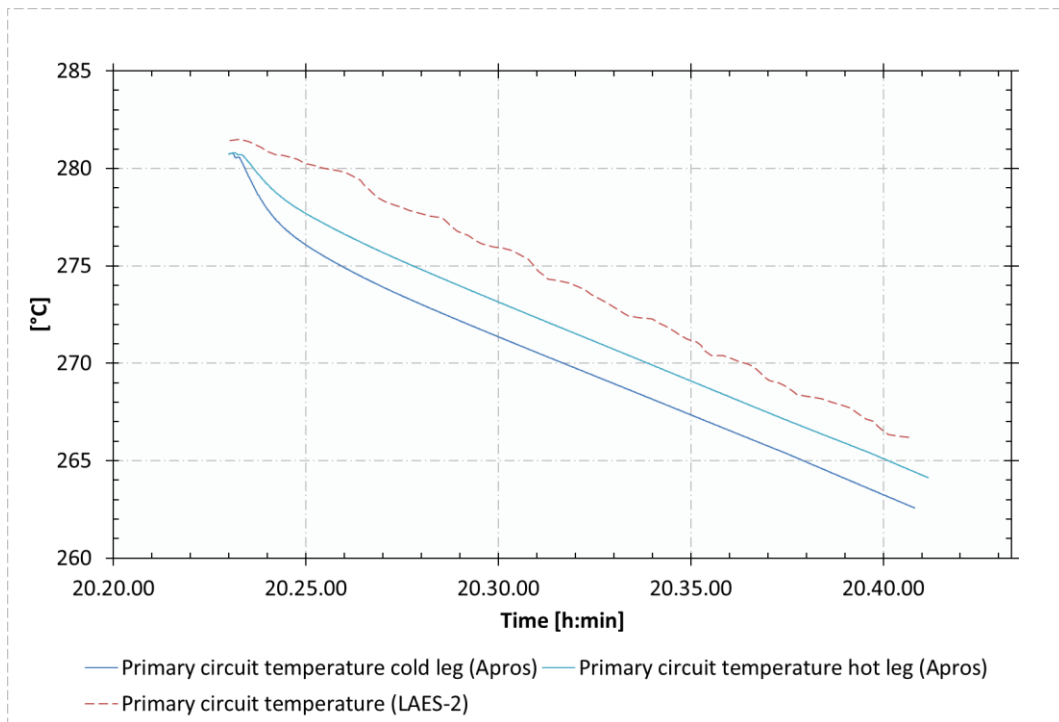


Figure 16: Primary circuit temperatures during test 2.

Test 3

The last test run for JNB system was test 3 in which the power and the mass flow through the system was decreased to design values when operating with the large starting valve. The system design power is 50 MW. To reach values close to this, the power was lowered from the maximum powers calculated during test 2 by reducing the mass flow. At LAES-II this was done by closing the manual control valve by approximately 30%. In Apros, the loss coefficients of all pipes and valves were returned to their default values and the pressure loss of the control valve was increased to 0.01 MPa. These changes allowed for the system to operate at design values and the test run 3 was completed. The results of this run are shown in Table 6.

Table 6: Results of test 3, large valve 70% open.

	Apros	LAES-II
Test duration (min)	7	7
Primary circuit temperature start (°C)	260.7	261.0
Primary circuit temperature end (°C)	255.9	256.0
SG1 pressure start (MPa)	4.65	4.60
SG1 pressure end (MPa)	4.28	3.85
PHRS tank 1 temperature start (°C)	38.7	52.7
PHRS tank 1 temperature end (°C)	41.9	59.9
Mass flow through JNB (kg/s)	21.0	20.9
JNB power (MWt)	50.3	50.3
Cooling rate (°C/h)	40.1	42.8

As can be seen from this table, the results are once again similar. The primary circuit temperatures are almost identical when comparing with the cold leg temperature of Apros (see Figure 17). The mass flow, power and cooling rates are also very close, and the PHRS tank temperature follows the expected trend where a smaller tank heats up quicker than a larger one even when taking into account the difference in temperature measurement location mentioned earlier. The trend figures for test 3 are in Appendix 1.

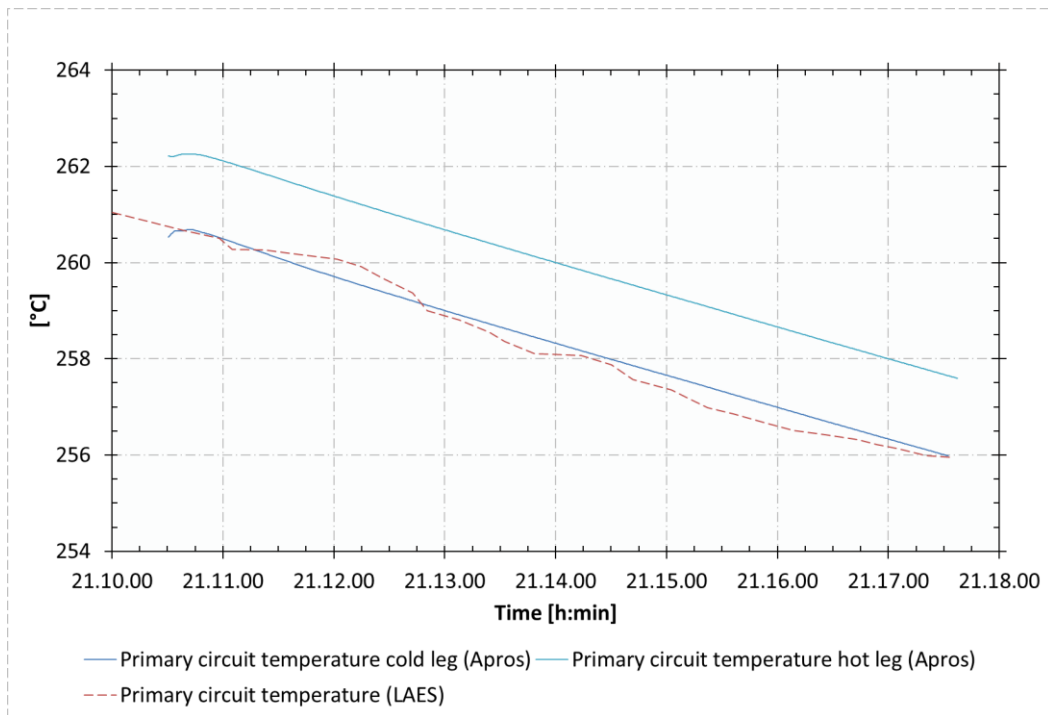


Figure 17: Primary circuit temperatures during test 3.

7.2 Containment passive heat removal system

7.2.1 Verification

The Verification of the CPHRS system was done in several steps. First the model was studied, and it was noted that it needed to be updated, as stated in the subsection 4.5.2. The JMP system's outlet line inside the sparger has a 50 mm hole which allows for liquid water to circulate out of the riser inside the sparger. This had not been modelled in the original Apros model and it was added to correct the representation of the model because this modification changes the flow behaviour of water inside the steam relief device.

This hole was modelled using a branch component with a diameter of 0.05 m and length of 0.004 m. Its form loss coefficient was set to 0, to allow for free flow out of the device. If losses were high on this component, it would hinder the start of natural circulation in the tank. The branch is connected

from the JMP outlet line to the volume inside the steam relief device both represented by different nodes in the Apros model.

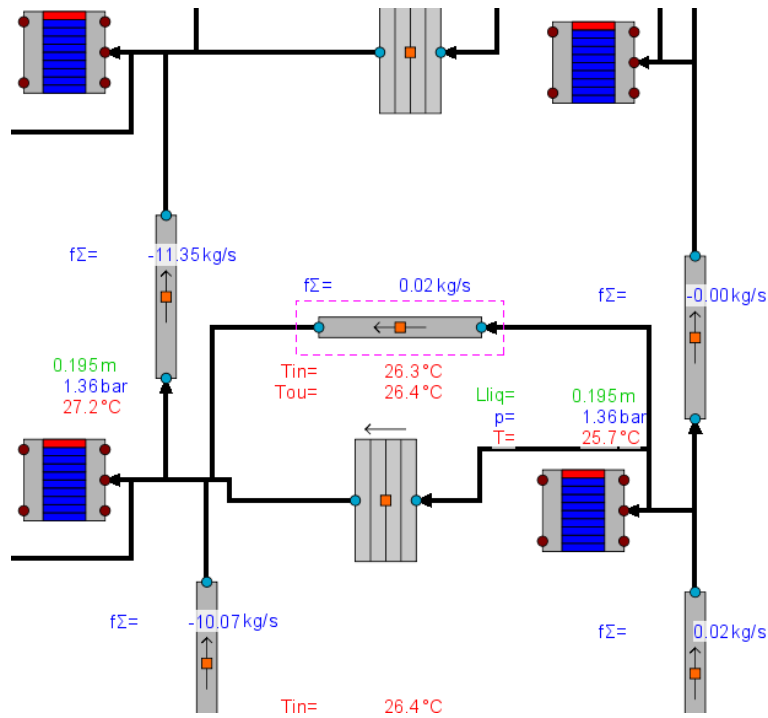


Figure 18: Hole in sparger's outlet line in Apros.

Next, Apros's CPHRS modelling capabilities were tested with a separate existing model. This was an Apros model of the Lappeenranta University of Technology's (LUT) PASI facility. The PASI is a test facility in Lappeenranta which houses a scaled down version of a single heat exchanger and cooling circuit of a VVER-1200 V-491 containment PHRS. This facility has been designed and constructed by the Nuclear Engineering research group of LUT as part of the INTEGRA project in the SAFIR2018 national nuclear power plant safety research programme. The objective of this facility is to conduct tests to measure the system's performance and to study the operation of a containment PHR system in detail. (Kouhia & Riikonen, 2018)

The PASI facility is designed to mimic the CPHRS of the Hanhikivi-1 power plant. The inlet and outlet lines are connected to a water tank to constitute

the heat removal circuit. The heat exchanger is housed in a pressure vessel to form conditions like the containment of a power plant. To achieve these conditions, steam can be fed to the vessel via a feeder system and an electrical heater can be used to heat the atmosphere inside. In Figure 19, the PASI facility and its main components are presented. (Kouhia & Riikonen, 2018)

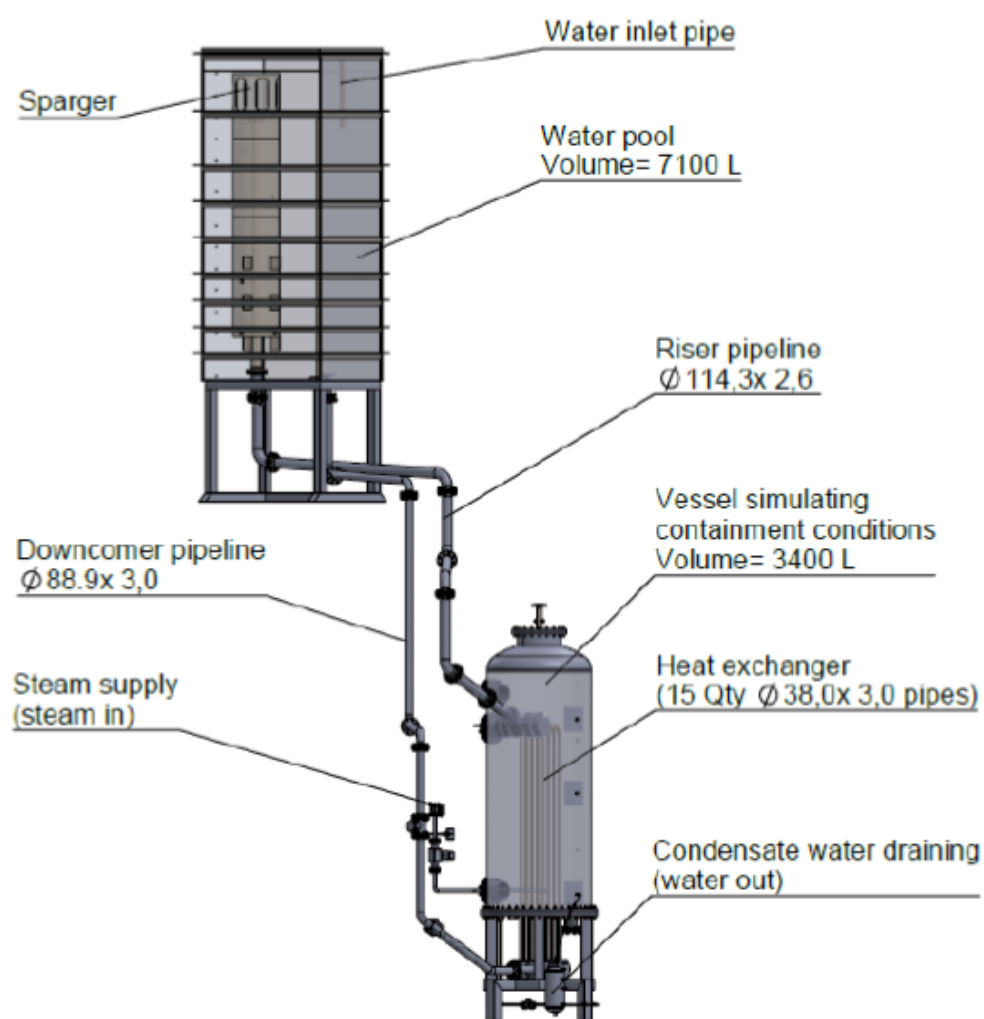


Figure 19: PASI test facility (Riikonen et al., 2021).

The PASI facility is of 1:2 height scale for the inlet and outlet lines and for the heat exchanger. The heat exchanger consists of 15 heat exchanging tubes.

These equate to a heat exchanging surface area of 4.02 m² (Riikonen et al., 2021). This is considerably smaller than compared to the reference plant where the area is 75.5 m² (Fennovoima Oy, 2020b). The ratio between the heat exchanging surface areas equal to 18.8.

In addition to the experiments made as part of the research programme, Fennovoima ordered a set of tests from LUT to be done with this facility. These tested the operation of the system and its heat transfer capacities. Included in these was an experiment whose specific objective was to mimic the conditions of the system in a power plant during commissioning tests. This was done by reaching and maintaining various quasi-steady states at different humidity levels. As these conditions are analogous to the conditions of the reference plant during its commissioning tests, it was deemed a good way to test Apros's modelling accuracy.

Therefore, preliminary test calculations were done with the PASI Apros model matching to the experiment made at the test facility. In these tests, the power of the heat exchanger was measured with different amounts of steam supplied to the vessel. At the start of the test, the heater was on and no steam was fed. The power stabilised to around 1 kW and humidity was 30%. The amount of steam supplied was then increased and the system allowed to stabilise to a quasi-steady state. This was done with steam amounts of 1 g/s, 2 g/s, 4 g/s and 6 g/s.

Some adjustments were made to the PASI Apros model so that it models the facility accurately during these specific tests. Firstly the, heat losses of the inlet and outlet lines and of the vessel had to be adjusted. They were set to approximately match the heat losses measured during the characterizing experiments of PASI facility. For the vessel temperatures of around 60 °C, the losses were approximately 0.7 kW. In addition, the heat transfer efficiencies of the heat exchanger were adjusted to match the values of the tests.

From previous testing, it was known that the heat transfer efficiencies of the heat exchanger had to be raised to values of over 100% so that the powers match to those of the test facility. This was again the case and the efficiency in this test was set to 210%. To explain this, there must be some inaccuracies in the Apros' calculation of heat transfer. Especially during condensation, it seems that Apros underestimates the amount of latent heat caused by the phase change. It was also tested to change the heat convection correlation in the PASI model to correlation 4, but this did not seem to influence the results and as such it was left to its default value of 1.

The tests were run, and the results can be seen in Table 7 and in Figure 20 and Figure 21.

Table 7: Results of PASI facility tests.

Steam supplied	Power (kW)		Humidity (%)	
	Apros	LUT	Apros	LUT
1 g/s	3.5	2.5	50	45
2 g/s	5.7	7.0	64	50-60
4 g/s	10.0	10.5	83	70-80
6 g/s	14.1	14.0	95	80-100

As can be seen from the table, the results are analogous. The power of the single heat exchanger in Apros follows well the power measured at the facility for different amounts of steam supplied. Furthermore, the humidity of the vessel that acts as the containment are also comparable. The humidity measurements had a margin of error of approx. $\pm 5\%$ which can explain some of the deviations.

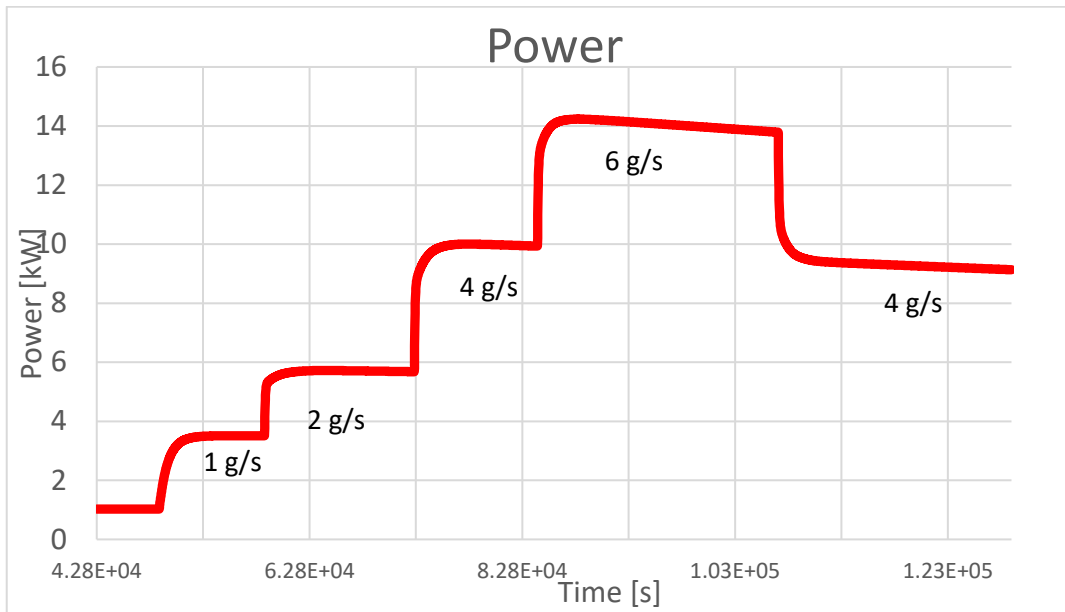


Figure 20: Apros calculation results with PASI facility model.

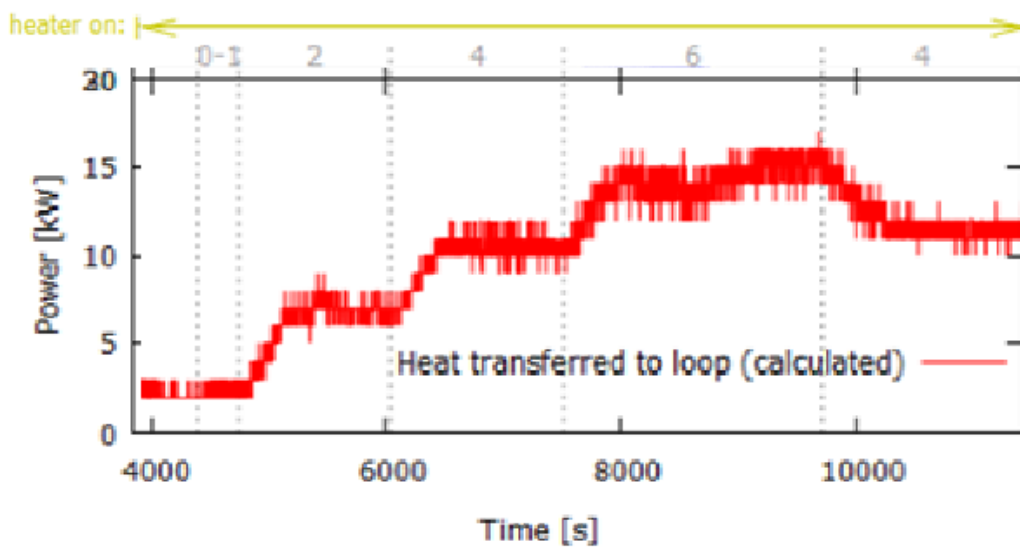


Figure 21: Results from the test conducted at the PASI facility (Riikonen et al., 2021).

Before starting the validation calculations with the full FH1 Apros model, the conditions of the containment were modified. The containment was heated up to the 56 °C as mentioned in (Geraghty et al., 2017). This was done by modifying the temperature directly from the nodes of the containment and starting the simulation to allow for it to stabilise. This took Apros a considerable amount of time as all the heat structures had to also heat up from the default 30 °C to 56 °C. To speed up this process, the heat structure components in Apros were modified to produce 1 MW of heat each. In addition, the temperature of the inflow air to the containment by the KLD10 system was raised to 55 °C and the KLA fans were left active to circulate air but their cooling was removed.

Additionally, a quick test was made to see the effect of the heat convection correlation change to the operation of this system. For the JNB system this change was pronounced and improved the quality of the results. For the JMP system however, the change was less prominent. An increase in system power of approx. 15 % ensued from the change with a small difference of 3 to 4 degrees for the heat exchangers inlet and outlet temperatures. It was decided to use the correlation 4, Churchill and Chu, also for the JMP system as it works by natural circulation. This means that free convection and turbulent flow characterise the situation in the JMP system the best.

7.2.2 Validation

The validation of the CPHRS system was done by comparing the results of the commissioning tests conducted at the reference plant (AO Rosenergoatom, 2017b) to calculations done with the Hanhikivi-1 Apros model. The results of the tests performed at the reference plant are presented per train tested in Table 8. Train 2 was not tested.

Table 8: Results of the CPHRS commissioning tests at LAES-II.

	Train 1	Train 3	Train 4
Water temperature HE inlet (°C)	23.0	22.7	23.1
Water temperature HE outlet (°C)	27.5	28.5	29.0
Difference in temperature outlet-inlet (°C)	4.5	5.8	6.9
Containment temperature start (°C)	56.1	56.0	56.0
Containment temperature end (°C)	55.5	55.3	55.1
Difference in temperature start-end (°C)	0.6	0.7	0.9
Mass flow through JMP (kg/s)	4.9	3.2	4.3
JMP power (kW)	90.6	79.4	104.2

The results of the commissioning tests between trains were similar but with differences. The mass flow was between 3.2 and 4.9 kg/s and the power varied between 79.4 kW and 104.2 kW. The capacity of the system seems to have a natural variation in results even though the trains themselves are identical and the conditions in the containment are reported to be the same.

To test the CPHRS in Apros, most of the systems in the model were excluded. This was done to speed up the calculation. Systems such as the reactor, the primary and the secondary circuit and the turbine were all excluded as they do not affect the operation of the CPHRS. Only the crucial processes and diagrams were left included. These were notably the processes of the passive heat removal systems and of the different containment volumes.

During the commissioning tests at the reference plant, the humidity present in the containment was unknown. It was stated that only a tiny amount of condensate had formed during the tests and thus the humidity must have been low. As no exact value is reported, a sensitivity analysis was done in Apros. This consisted of testing the system with different values of

containment humidity to see how it affects the results and what humidity would match the closest to the results from the reference plant.

The system was run with different amounts of humidity in the containment with the humidity being adjusted by Forced Feed Source containment components in Apros. The temperature of the containment remained approximately the same at 56 °C and the temperature at HE inlet was 25 °C. During the run, parameters important for examining the heat transfer were tracked. These were water temperature at outlet of heat exchangers, mass flow through JMP and power of JMP. The results of the analysis are shown in Table 9.

Table 9: Results of sensitivity analysis.

Humidity (%)	HE outlet temperature (°C)	Mass flow (kg/s)	Power (kW)
20	30.1	2.8	56.1
25	30.6	2.9	66.7
30	31.2	3.1	87.5
35	32.1	3.4	105.1
40	33.8	3.9	112.2
45	34.2	4.0	140.9
50	35.1	4.1	167.5

As can be seen from the table, the humidity affects the results significantly. At a lower humidity, the outlet temperature and mass flow are smaller which also equates to smaller system power. This is explained by condensation on the heat exchangers generating a considerable part of the heat transfer of the system. At lower humidity, less water is present in the air of the containment and thus less condensation can take place which translates to a decreased heat transfer.

Examining the results of the sensitivity analysis, the closest result in terms of power of the system to the commissioning tests is at 30% humidity. In the tests at LAES-II, the power calculated was 80-100 kW depending on the train which means that the humidity was probably around 30 to 35%. Regarding the mass flow through the system, for trains 1 and 4 it was considerably higher than in Apros for the specific power. However, the mass flow for train 3 matched with Apros results. The results for train 3 are the lowest between the trains and therefore the most conservative. Thus, a specific test run in Apros is made at 30% humidity with its results compared with the LAES-II results for train 3. This is presented in Table 10.

Table 10: Results of CPHRS validation test.

	Apros	LAES-II (train 3)
Test duration (min)	120	120
Water temperature HE inlet (°C)	25.4	22.7
Water temperature HE outlet (°C)	31.6	28.5
Difference in temperature outlet-inlet (°C)	6.2	5.8
Containment temperature start (°C)	57.1	56.0
Containment temperature end (°C)	56.2	55.3
Difference in temperature start-end (°C)	0.9	0.7
Mass flow through JMP (kg/s)	3.2	3.2
JMP power (kW)	88.6	79.4

As can be seen from the table, the starting conditions were similar. The containment was at 56 °C and the PHRS tank temperature was close at 23 to 25 °C. The test calculation was started by opening the shut-off valves JMP10AA801 and JMP10AA802. This started the operation of the system as the water in the heat exchangers was warmer than in the outlet line which induced natural convection. The warm water rose upwards towards the

PHRS tank and cooler water flowed down from the tank through the inlet line to the heat exchangers.

At the start of the test, some instabilities were in place caused by temperature differences in the lines and the surfaces. This caused strong oscillations in mass flow through the system. The flow fluctuated between 4 kg/s and 10 kg/s. At the same time the water temperature at the heat exchanger outlet rose in both tests to around 52 °C due to warm water being trapped in the system. After approximately 10 minutes of operation, the system stabilised. The flow through the system settled to 3.2 kg/s in both tests and the HE outlet temperature to 28.5 °C at LAES-II and 31.6 °C in Apros (see Figure 22).

Overall, the results were similar with water temperature from inlet to outlet line (ΔT) heats up by 6.2 °C in Apros compared to the 5.8 °C at LAES-II. The mass flow was identical and the power of the system only approx. 9 kW apart. The trend figures for these results can be found in Appendix 2.

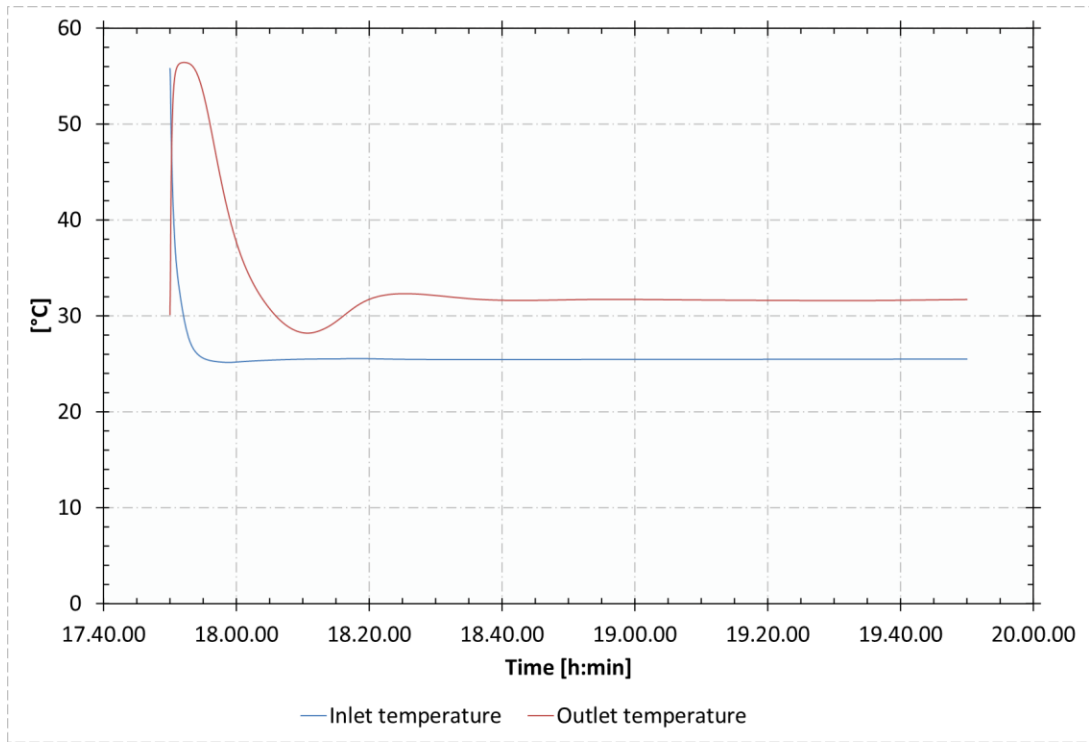


Figure 22: Water temperatures at HE inlet and outlet in Apros.

8 DISCUSSION

8.1 Steam generator passive heat removal system

As an outcome of the verification process for the SG PHRS, the model was updated to include the headers of the heat exchangers which increased the total heat exchanging surface. Additionally, the nodes of the PHRS tank and their height in relation to the components inside the tank was adjusted according to newer design information. Finally, the heat convection correlation was changed to correlation 4 (mixed free and forced convection) and preliminary testing with this option showed good results that were in line with commissioning test results.

The results of the validation calculations showed that Apros results match well with commissioning tests results. The mass flow, power and cooling rates were all similar. The most noticeable difference in JNB test results is in SG1 pressure. At LAES-II the end pressure was consistently lower by 0.20 to 0.43 MPa. This was a pattern that could be seen in all test runs: the SG pressure at the reference plant is decreased by the JNB system more effectively than in Apros.

No exact reason for the pressure variation can be identified from these tests. The BRU-A which were used to control the pressure in the secondary side were closed in both Apros and LAES-II before the start of the tests. The MSIVs were also closed in Apros and while it was not directly stated, these are expected to be also closed at the reference plant as they would allow for steam to escape from the SG to the MSH and the turbine. As the reason for this small discrepancy could not be identified this is something that could be studied further if new data on this system becomes available.

To summarise, the results of the verification and validation process for the JNB system, the Apros model of the JNB system has been built well and models the system accurately. The difference stated earlier is small enough that it would not affect the usability of the model. In addition, the difference is that the pressure is higher in Apros, which makes the model more conservative, which is preferred in safety analyses.

8.2 Containment passive heat removal system

For the CPHRS, the verification process led to the addition of the sparger hole to the model. During the verification, preliminary calculations were also done comparing the results of the PASI Apros model to the results of the facility itself. These tests were done to evaluate the heat transfer modelling of Apros. The results of these tests showed that the heat transfer of Apros matches that of the facility when using a heat transfer efficiency of 210% for the single heat exchanger. The reason for such a high efficiency seems to be due to inaccuracies in condensation heat transfer for that specific model and do not appear to affect the complete plant model. This however still requires closer investigation.

In the validation process for the CPHRS, firstly, a sensitivity analysis was performed to see the effect humidity has on the system performance. This effect was significant, and it was deducted that the humidity at LAES-II during the commissioning tests was probably approximately 30%. With this result, a specific test calculation was done with the FH1 Apros model at 30% humidity and its results compared with the results of the commissioning test.

The results of Apros were similar to those of the commissioning tests and matched almost perfectly with the results of LAES-II train 3. The mass flow was identical at 3.2 kg/s, and the power of the system was close with a difference of only 9 kW. This difference may be caused by the slightly higher

temperature in the containment or due to the humidity not being exactly the same. The change in temperature between the heat exchanger inlet and outlet was also nearly matched with a ΔT of 6.2 °C in Apros and 5.8 °C at LAES-II. Therefore, it can be said that the Apros model of the JMP system is built well and models the operation of the system precisely.

The reason for the discrepancy between the two results is unclear. The difference in mass flow through the JMP system could be explained by pressure losses and friction coefficients being different as there is no information from the reference plant, and they are only estimated in Apros. Nonetheless, the larger factor for inaccuracies are the conditions inside the containment such as the humidity and the temperature. These affect the operation of the system greatly. As the exact humidity at LAES-II is not reported and the temperature is approximate, the conditions of the Apros model had to be estimated. As already a small difference affects the JMP system it affects the accuracy at which a validation can be made.

The imprecisions in temperature and humidity were small and therefore the results were deemed acceptable. While differences in exact values persisted, the JMP system operated close to the same power in both tests. The mass flow was identical and the water temperature change difference is small enough that they do not affect the results nor the usability of the model negatively.

8.3 Limitations

The possibility to conduct an accurate verification and validation process rests on the availability of credible data. With this research the data availability in general was limited with only two sets of test results from the reference plant commissioning tests were received from the Supplier. These two

were then used for validation as they are the only available data from a real nuclear power plant.

For the SG PHRS, this data was of relatively good quality and showed mass flows and heat flows through the system that were akin to the design capacity. However, some information was missing, and the exact measurement locations were not specified which brought uncertainty to the process. The results for the SG PHRS allowed nonetheless to perform validation comparisons that were mostly precise.

For the CPHRS, the results of the commissioning tests had similar problems. They were lacking information such as humidity and pressure inside the containment which lowers the quality of validation possible. Additionally, the tests were performed in conditions that did not test the design capacity of the system. From the sensitivity analysis it does seem that the model works well also at higher concentrations of humidity and temperature, but this should be studied further. Nonetheless, the results calculated in Apros were similar to the LAES-II results and thus a validation could be made.

8.4 Recommendations

This thesis suggests recommendations for the future use of Apros model. Firstly, the model changes made improved the accuracy of the system models and should be replicated to the other trains. These were the headers, the sparger hole, and the updated nodes of the PHRS tanks. Secondly, the heat convection correlation for the calculation of heat transfer for the passive heat removal systems should be changed. The Dittus-Boelter forced convection correlation is a good option for most parts of the model but as the PHRSs function using natural convection, the Churchill and Chu mixed free and forced convection correlation should be used for them. In the next version of

Apros 6.11, the correlation can be set individually for diagrams/systems and this is recommended for the two passive heat removal systems.

8.5 Future work

For the two systems studied, some future research suggestions are made. The steam generator passive heat removal system's model was deemed accurate but the difference in steam generator pressure was something that could be studied further if more data becomes available on this system. To the containment passive heat removal system model more validation should be performed with conditions closer to design values. The possibility for additional validation is, however, limited by data availability.

Regarding the rest of the Hanhikivi-1 plant model, V&V work should be continued. To ensure the correct functioning of the complete simulation model, a V&V should be conducted for the entire model or separately for each system. With this, the credibility of the model and thus of the safety analyses done for the FH1 Construction License Application and Operating License Application is increased as a proof of validity exists. It is however important to note that the possibility to conduct such V&Vs is limited by the amount of data available from the Supplier. The more data received from the commissioning tests and operational phase of the reference plant, the more thorough V&V processes can be done for the simulation model.

9 CONCLUSIONS

Passive heat removal systems are a new kind of safety system used in many generation III+ nuclear reactor designs to increase the safety of the plant. This is also the case for Fennovoima's upcoming Hanhikivi-1 nuclear power plant to be built in the municipality of Pyhäjoki. As these systems are new, with only a handful of operating plants with such systems, the experience in building simulation models for them is limited. In this thesis, the simulation models in Apros of two PHRS systems of a VVER-1200 V-491 type pressurized water reactor were verified and validated. The motivation behind this research was to study the Hanhikivi-1 Apros model and how well it simulates these systems.

The verification and validation process was done for both the steam generator and the containment passive heat removal systems. The verification included studying the model, modifying it in order to fix inaccuracies and performing preliminary calculations. The validation process in the other hand was to compare the results of the model with data from the reference plant to quantify the accuracy of the model output.

Main takeaways from this V&V study were that the steam generator passive heat removal system model built in Apros is sufficiently accurate and its output follows well the results from the reference plant with a small margin of error. However, to achieve this, it is recommended to change the heat convection correlation in Apros from the default Dittus-Boelter to the Churchill and Chu mixed free and forced convection correlation. This latter depicts the situation especially on the outer surfaces of the heat exchangers better and thus allow for more accurate results.

Regarding the containment passive heat removal system, the preliminary calculations of the verification process with the PASI model showed that Apros

does model CPHRSs well. Next, sensitivity analysis and validation calculations were done with the plant model and these matched to the results from the commissioning tests of the reference plant to the needed degree. Some differences in mass flow and temperatures inside the system were in place but these were small enough and thus the results are deemed to be acceptable. Therefore, the Apros model of the CPHRS is sufficiently accurate and models the system well.

REFERENCES

- AO Rosenergoatom. (2017a). *Report on the Test of System of PHR through Steam Generators LNPP-2*. Sosnovy Bor, Russia.
- AO Rosenergoatom. (2017b). *Report on the Test of Containment PHRS LNPP-2*. Sosnovy Bor, Russia.
- Balci, O. (1997). Verification, Validation and Accreditation of Simulation Models. *Winter Simulation Conference*, (pp. 135-141). Atlanta, GE, USA.
- Carson, J. S. (2002). Model Verification and Validation. *Winter Simulation Conference* (pp. 52-58). Marietta, GA: Brooks-PRI Automation.
- Fennovoima Oy. (2020a). *FH1 PSAR 6.7.4 Steam Generator Passive Heat Removal System (JNB)*. Preliminary Safety Analysis Report, Helsinki.
- Fennovoima Oy. (2020b). *FH1 PSAR 6.2.3 Containment Passive Heat Removal System (JMP)*. Preliminary Safety Analysis Report, Helsinki.
- Fennovoima Oy. (2021, March 5). Hanhikivi-1 Apros model. Helsinki.
- Fortum & VTT. (n.d.). *Apros Datasheet: 1D- and 3D-Neutronics models*. Espoo. Retrieved from https://www.apros.fi/wp-content/uploads/sites/27/2020/09/205-Apros_Datasheet_1D-_and_3D-Neutronics_Models.pdf
- Fortum & VTT. (n.d.). *Apros Datasheet: Thermal Hydraulics Modelling*. Espoo. Retrieved from <https://www.apros.fi/product-information/white-papers/>
- Geraghty, M., Stålhandske, K., Kuzin, S., Rintala, J., Vahero, J., & Rumin, A. (2017). *LAES II Passive Heat Removal System (PHRS) Commissioning Tests*. Helsinki: Fennovoima Oy.
- IAEA. (1991). *Safety Related Terms for Advanced Nuclear Plants*. Vienna, Austria: International Atomic Energy Agency. Retrieved from

https://www-pub.iaea.org/MTCD/publications/PDF/te_626_web.pdf

- IAEA. (2000). *Safety of Nuclear Power Plants: Design*. Vienna: International Atomic Energy Agency.
- IAEA. (2009). *Passive Safety Systems and Natural Circulation in Water Cooled Nuclear Power Plants*. Vienna, Austria: International Atomic Energy Agency. Retrieved from https://www-pub.iaea.org/MTCD/Publications/PDF/te_1624_web.pdf
- Incropera, F. P., Dewitt, D. P., Bergman, T. L., & Lavine, A. S. (2006). *Fundamentals of Heat and Mass Transfer* (6th ed.). Hoboken, NJ: John Wiley & Sons.
- JSC Atomproekt. (2020). *Initial Data for Deterministic Safety Analysis*. FH1.B.P000.1.&&&&&.021.JE.0001.E.
- Kouhia, V., & Riikonen, V. (2018). *PASI facility – characterizing experiments*. INTEGRA 3/2018, Lappeenranta University of Technology, Nuclear Engineering, Lappeenranta.
- Kurki, J., Ylijoki, J., & Leskinen, J. (2019). *The Constitutive Equations of the Two-Fluid Model*. Espoo: VTT.
- Lamarsh, J. R., & Baratta, A. J. (2001). *Introduction to Nuclear Engineering* (3rd ed.). New Jersey, NJ, USA: Prentice-Hall.
- MITRE Corporation. (2013, August 28). *Verification and Validation of Simulation Models*. Retrieved February 10, 2021, from MITRE Corporation Web site: <https://www.mitre.org/publications/systems-engineering-guide/se-lifecycle-building-blocks/other-se-lifecycle-building-blocks-articles/verification-and-validation-of-simulation-models>
- Naylor, T. H., & Finger, J. M. (1967, October). Verification of Computer Simulation Models. *Management Science*, 14(2), pp. B92-B105.
- Peltokorpi, L., & Hongisto, O. (2020). *Apros Model Description, version 4.0*. Espoo: Fortum.

- Puska, E. K., Rintala, J., Kurki, J., & Leskinen, J. (2015). *Three-dimensional Neutronics Model User's Guide*. Espoo: VTT, latest revision in July 2020.
- Riikonen, V., Pyy, L., Kouhia, V., Räsänen, A., Kotro, E., & Tielinen, K. (2021). *Second Part of the PASI Experiments for Fennovoima*. Research Report, LUT University, Nuclear Engineering, Lappeenranta.
- Sargent, R. G. (1988). A Tutorial on Validation and Verification of Simulation Models. *Winter Simulation Conference*, (pp. 33-39). San Diego, CA, USA.
- Sargent, R. G. (2011). Verification and Validation of Simulation Models. *Winter Simulation Conference*, (pp. 183-198). Phoenix, AZ, USA.
- Sargent, R. G. (2015). An Introductory Tutorial on Verification and Validation of Simulation Models. *Winter Simulation Conference*, (pp. 1729-1740). Huntington Beach, CA, USA.
- Sargent, R. G. (2020). Verification and Validation of Simulation Models: An Advanced Tutorial. *Winter Simulation Conference*, (pp. 16-29). Virtual Conference.
- Sargent, R. G., & Balci, O. (2017). History of Verification and Validation of Simulation Models. *Winter Simulation Conference*, (pp. 292-307). Las Vegas, NV, USA.
- Schulz, T. (2006, August). Westinghouse AP1000 advanced passive plant. *Nuclear Engineering and Design*, 236(14-16), pp. 1547-1557.
- Silde, A., & Ylijoki, J. (2020a). *Nuclear Power Plant Containment Model user's guide*. VTT, Espoo.
- Silde, A., & Ylijoki, J. (2020b). *Nuclear Power Plant Containment Model of APROS 6.09 description of code models*. VTT, Espoo.
- State Atomic Energy Corporation ROSATOM. (2013). *The VVER Today*. Moscow, Russia. Retrieved February 2021, from

<https://rosatom.ru/upload/iblock/obe/obe1220af25741375138ecd1afb18743.pdf>

Thacker, B., Doebling, S., Henez, F., Anderson, M., Pepin, J., & Rodriguez, E. (2004). *Concepts of Model Verification and Validation*. Los Alamos, NM: Los Alamos National Laboratory.

Tsang, C.-F. (1990). *The Modeling Process and Model Validation*. University of California, Lawrence Berkeley Laboratory, Earth Sciences Division, Berkeley, CA, USA.

Winton, C. (2008). *Verification and Validation of Simulation Models*. Jacksonville, FL, USA: University of North Florida. Retrieved from https://www.unf.edu/~cwinton/html/cop4300/s09/class.notes/VerifyValidate_ppt.pdf

World Nuclear Association. (2020, September). *Advanced Nuclear Power Reactors*. Retrieved February 2021, from World Nuclear Association: <https://www.world-nuclear.org/information-library/nuclear-fuel-cycle/nuclear-power-reactors/advanced-nuclear-power-reactors.aspx>

World Nuclear Association. (2021, January). *Nuclear Power in Russia*. Retrieved February 10, 2021, from World Nuclear Association: <https://www.world-nuclear.org/information-library/country-profiles/countries-o-s/russia-nuclear-power.aspx>

Ylijoki, J., Karppinen, I., Puska, E.-K., Silde, A., Porkholm, K., & Kontio, H. (2015). *APROS Validation: Selected Validation Cases Related to Nuclear Safety Analyses and Training Simulators*. Espoo: VTT & Fortum. Retrieved from https://www.apros.fi/wp-content/uploads/sites/27/2020/09/189-Validation_cases_list.pdf

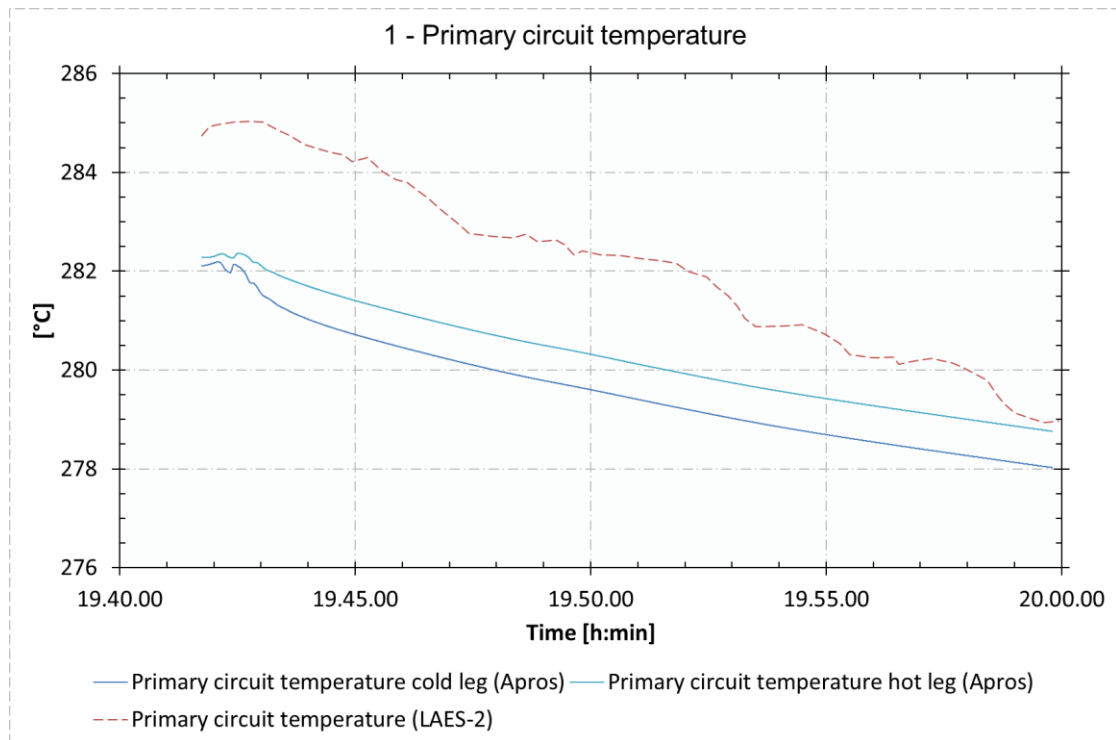
Zein, T. (2020, December). *FH1 Primary Circuit*. Helsinki: Fennovoima Oy.

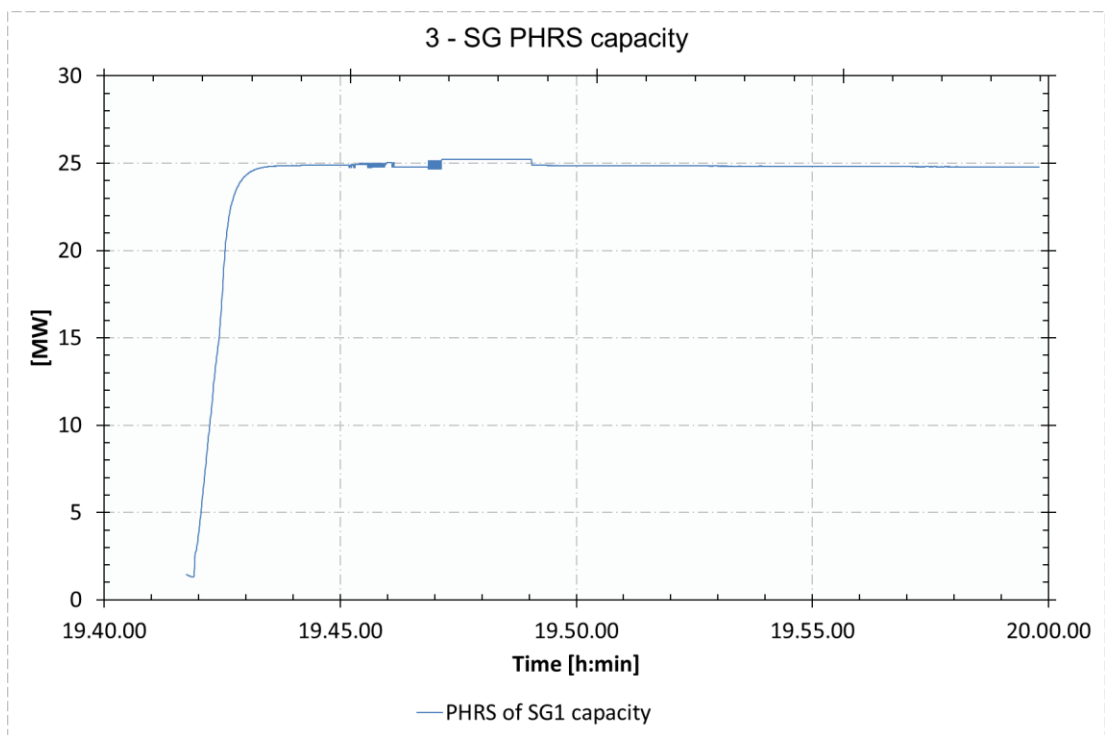
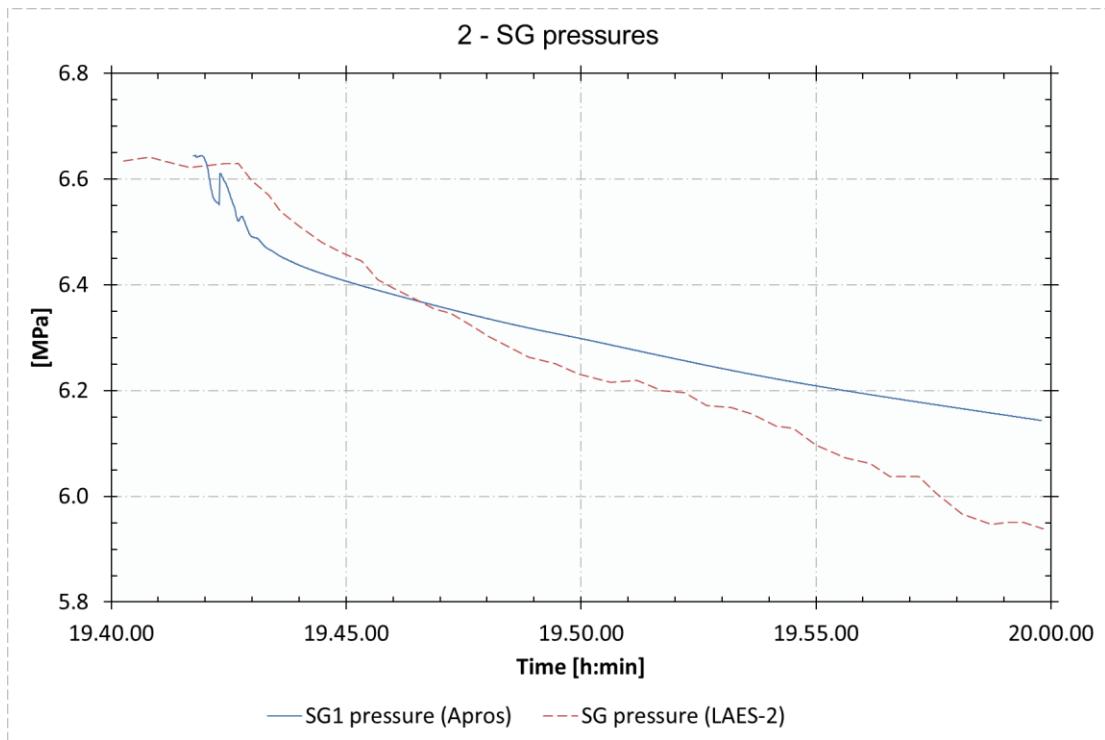
APPENDICES

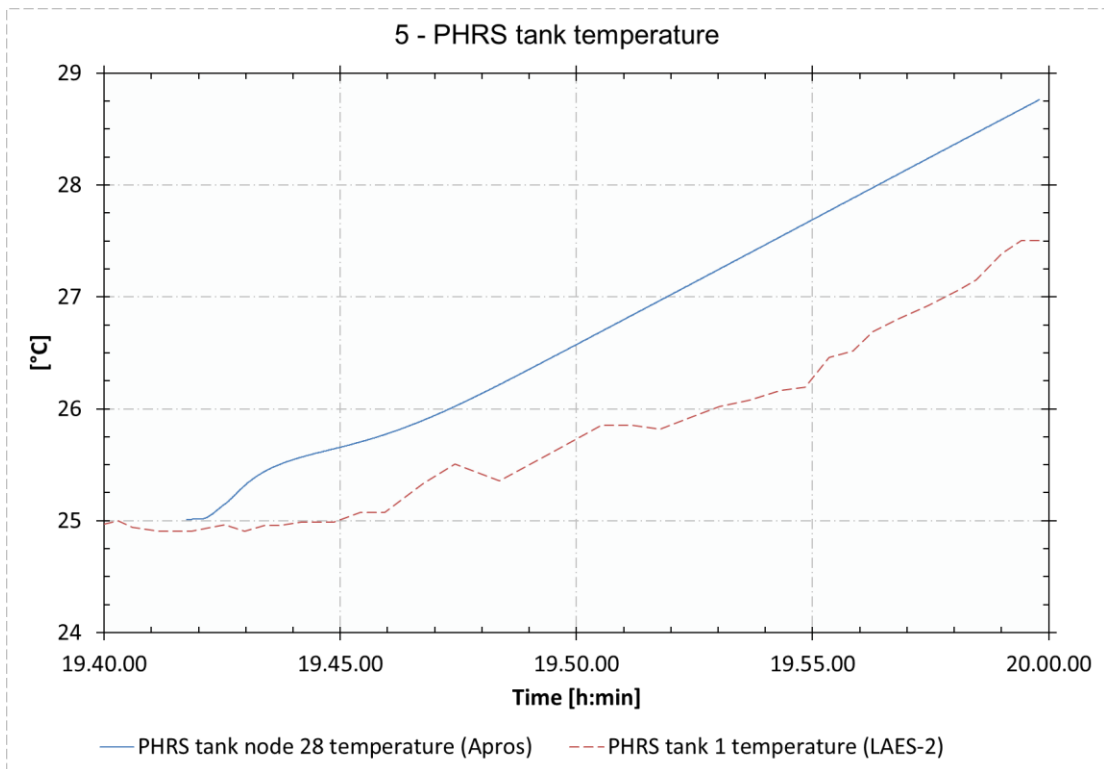
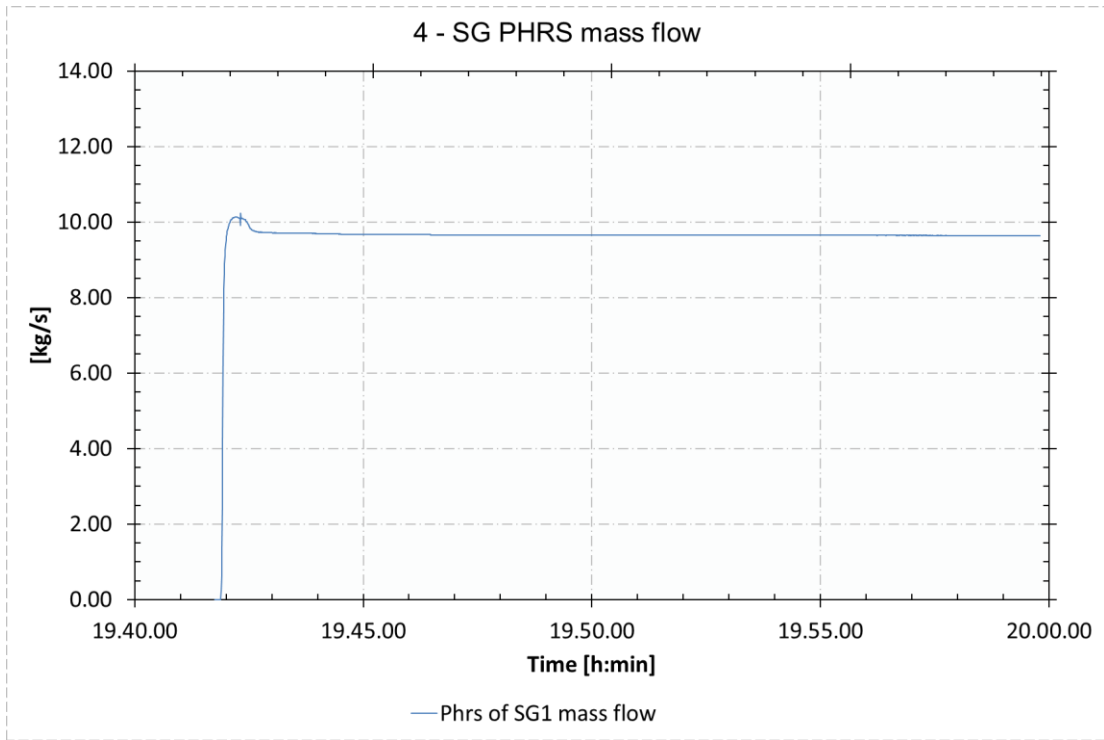
Appendix 1: Trend figures SG PHRS

The results for the steam generator passive heat removal system validation calculations for the three test runs (see subsection 7.1.2) are presented in this Appendix.

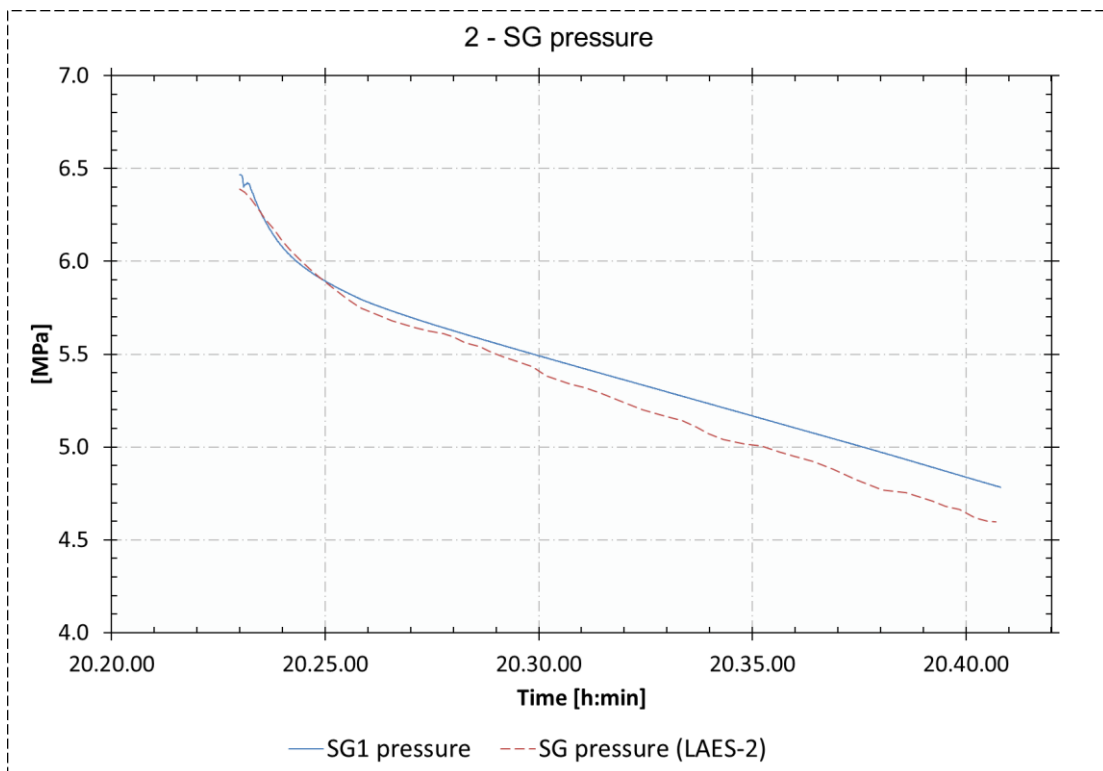
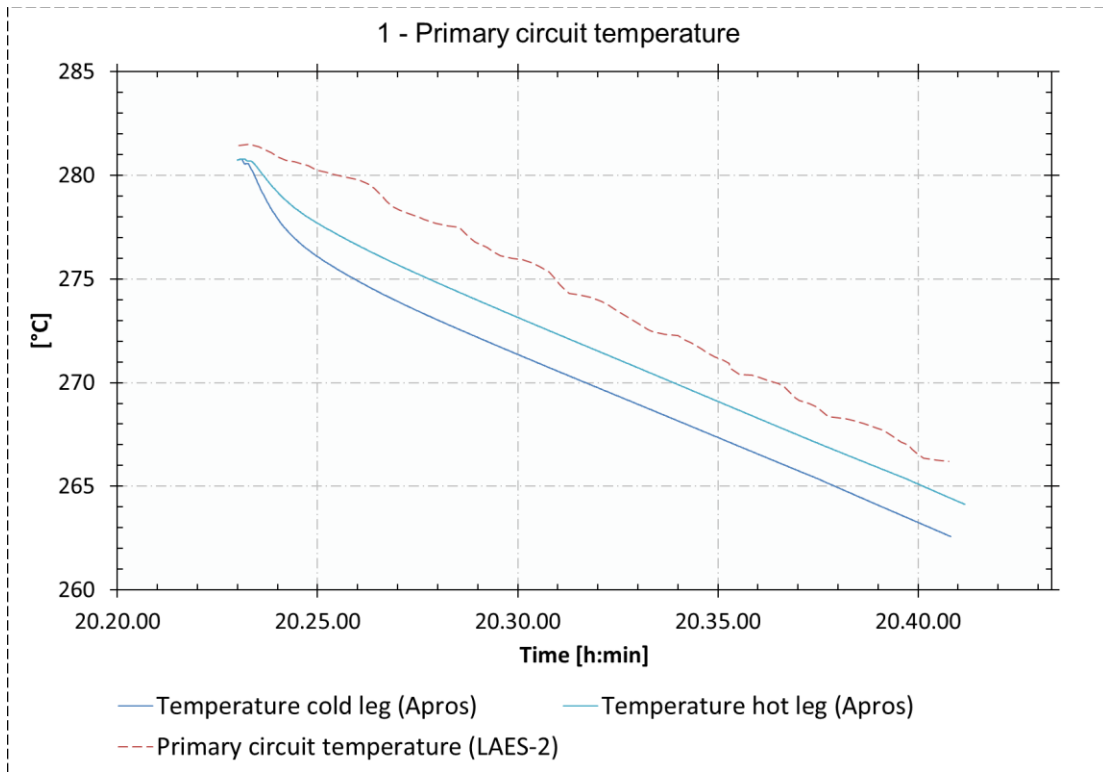
Test 1

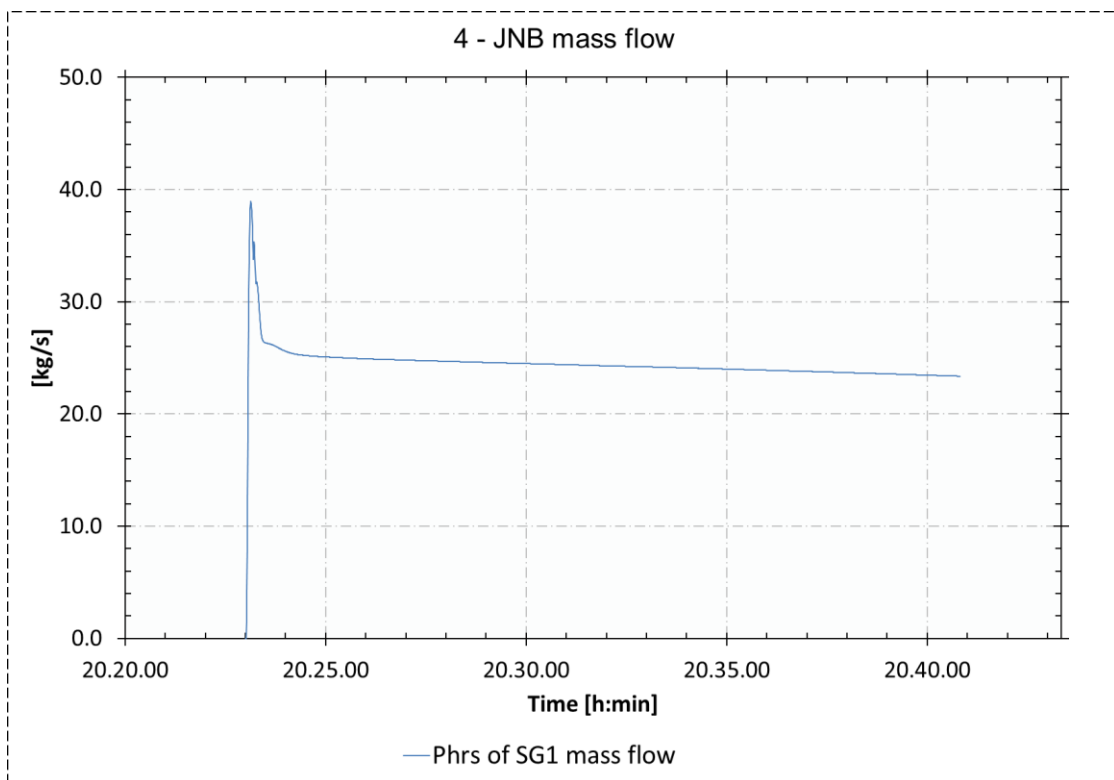
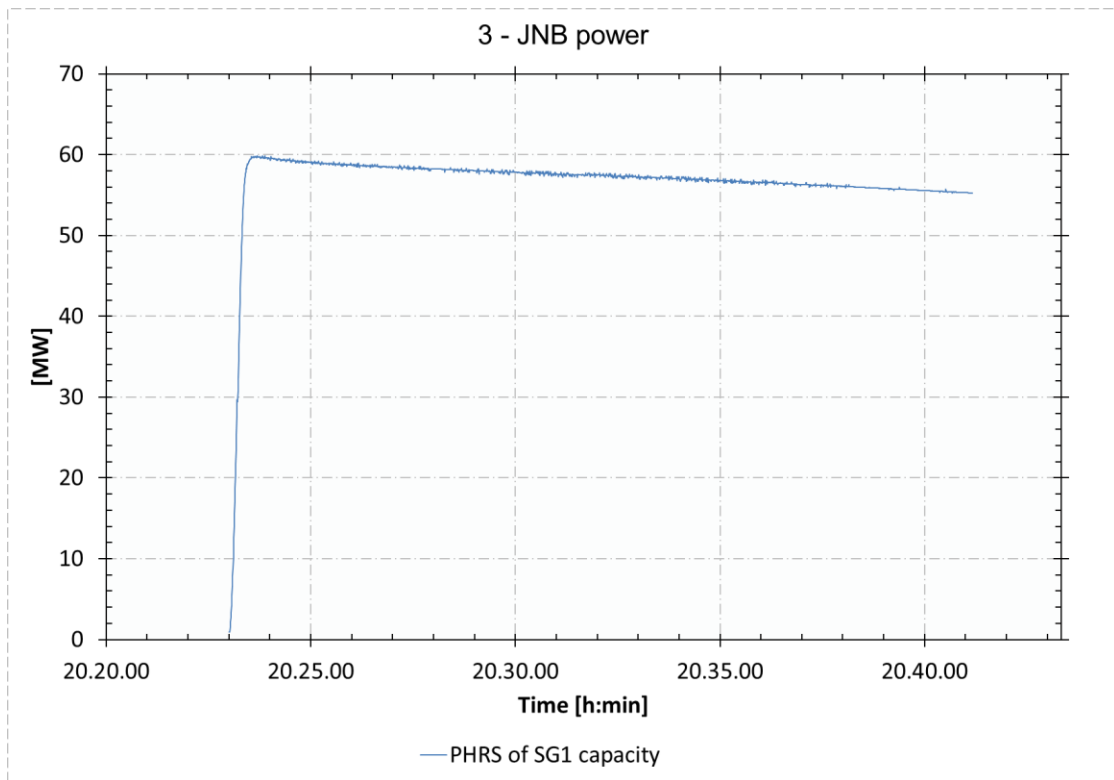


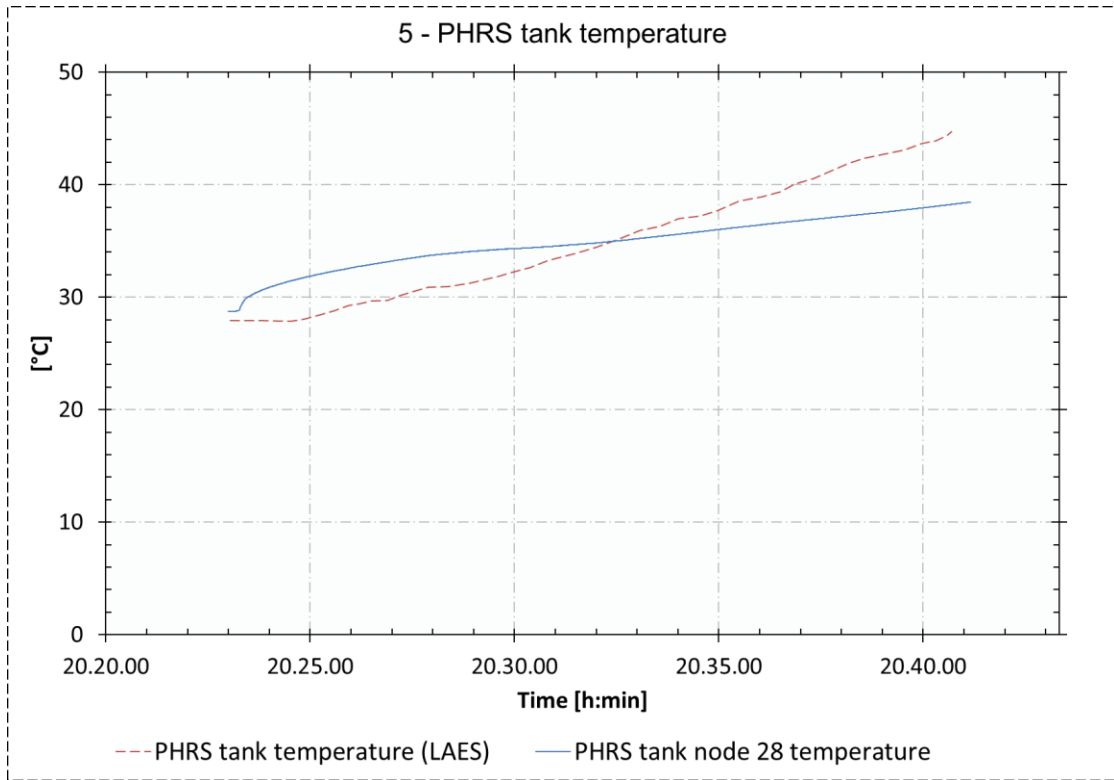




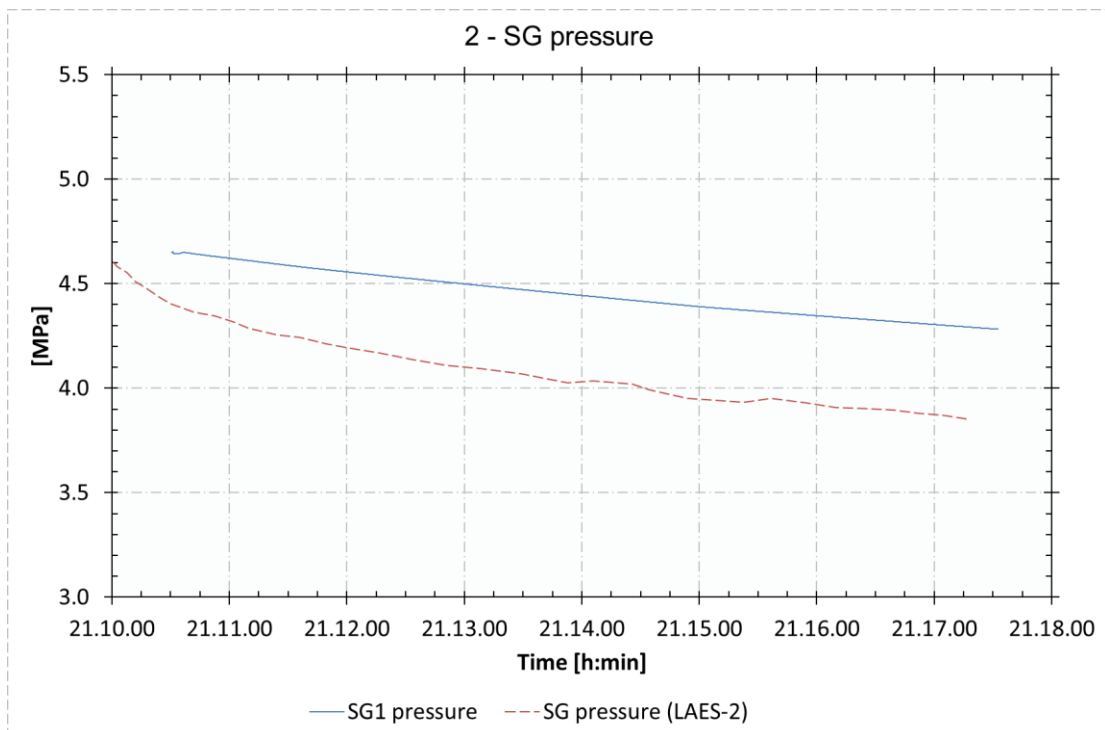
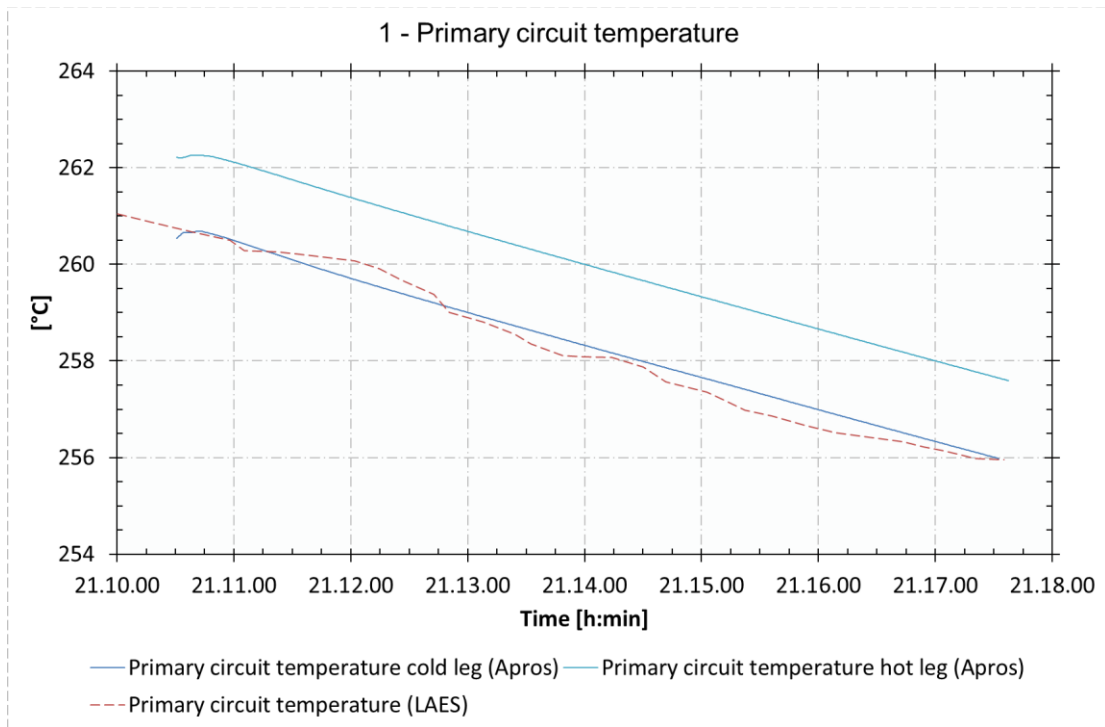
Test 2

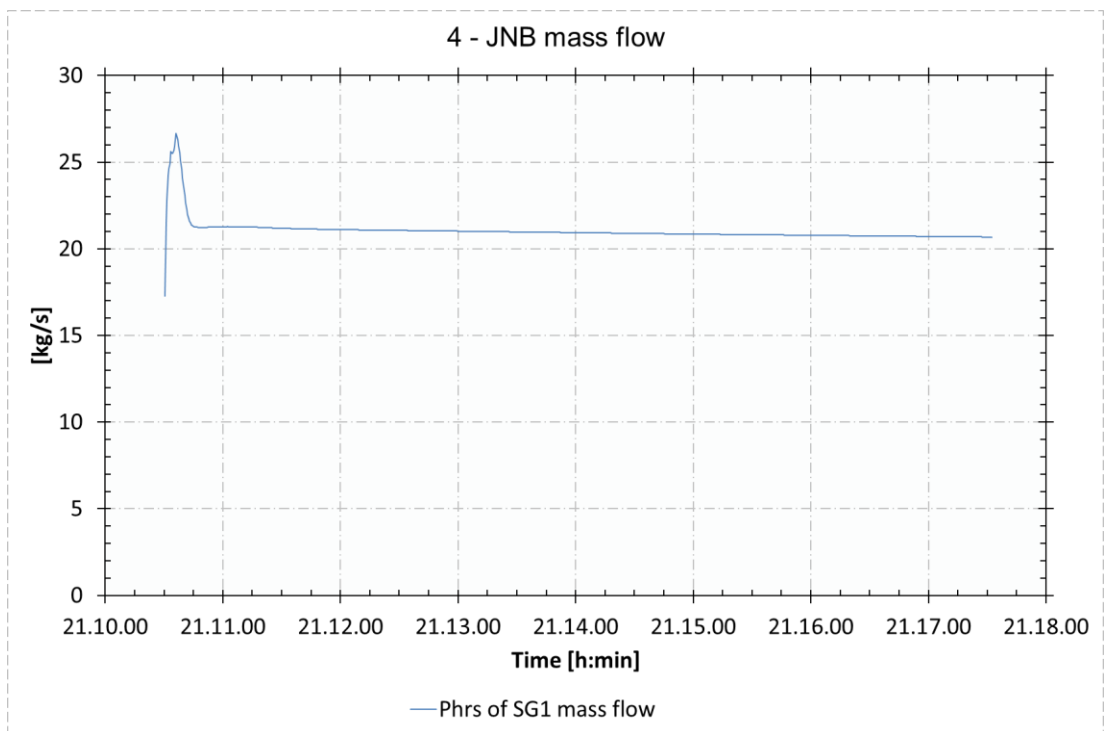
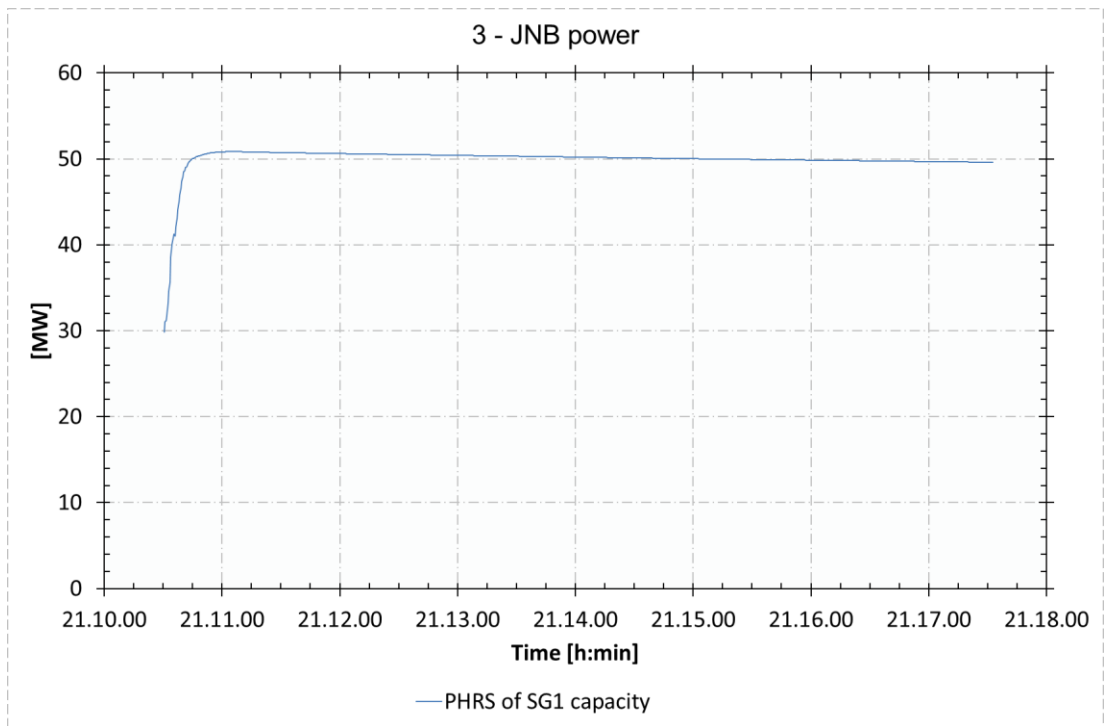


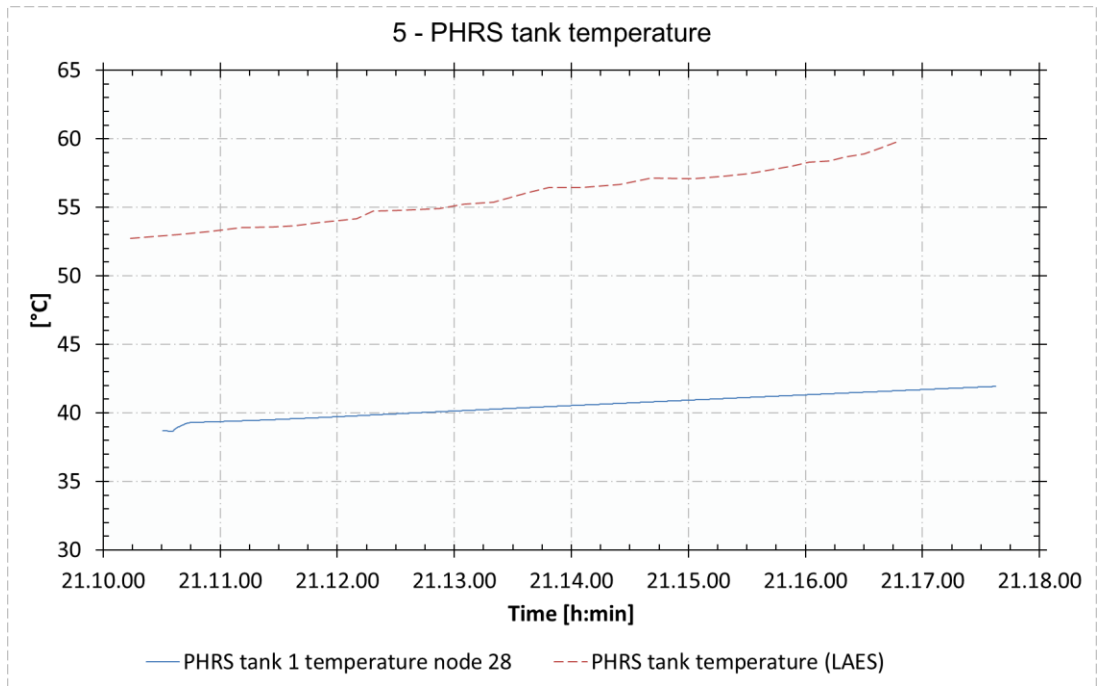




Test 3







Appendix 2: Trend figures CPHRS

The results for the containment passive heat removal system validation calculations (see subsection 7.2.2) are presented in this Appendix.

